

10 July 2017

Dear Editor:

Please find enclosed for a revised manuscript entitled "*Coupling a three-dimensional subsurface flow and transport model with a land surface model to simulate stream-aquifer-land interactions (CP v1.0)*" which I am submitting for consideration of publication as a model description paper in Geoscientific Model Development.

Significant modifications have been made in the revised version compared to the original submission and are summarized as follows:

1. The model name has been changed from PFLOTRAN\_CLM v1.0 to CP v1.0 to address the concern from reviewers on the coupling sequence and potential overlap with existing models;
2. The model coupling section (section 2.3) has been thoroughly revised to answer questions from the reviewers;
3. The introduction section (section 1) has been revised to include recent developments in the field and to provide stronger scientific motivations for developing a coupled model;
4. Detailed discussions on limitations of CP v1.0 are added to section 5 of the revised manuscript.
5. Additional figures are provided, and the original figures are revised in response to reviewers' comments.
6. The code availability section has been revised to include publicly accessible repositories for the model codes, tutorial, driving scripts, and datasets used in the paper.

We sincerely hope that the revisions could make the manuscript suitable for publication in Geoscientific Model Development. Thanks for your consideration and we look forward to hearing from you.

Sincerely,

*Maoyi Huang*

Maoyi Huang, Ph.D.  
Staff Scientist  
Atmospheric Sciences and Global Change Division  
Pacific Northwest National Laboratory

# **Coupling a three-dimensional subsurface flow and transport model with a land surface model to simulate stream-aquifer-land interactions (CPv1.0) [MS No.: gmd-2017-35]**

## **Responses to review comments**

### Anonymous Referee #1:

*The authors present a new coupled version of CLM4.5 and PFLOTRAN, and demonstrate the impacts of resolution, horizontal fluxes, and river stage height in simulating groundwater levels and turbulent fluxes between the land and the atmosphere.*

*The authors demonstrate that the new model is capable of simulating the observed water table depth, independent of the model resolution. The authors show PF-CLM results when there is no lateral subsurface exchange. Does this produce the exact same results as CLM without PFLOTRAN? If not CLM should be included in the manuscript. If so the authors should state that running PF-CLM without horizontal transfer gives identical results to CLM.*

#### Response:

Thanks for the suggestion. We understand that the standalone CLM4.5 could serve as a good reference for most readers. Therefore, we have included a figure from the CLM4.5 simulation in the supplementary material (i.e., Figure S4) and added discussions on differences in lines 415-427 of the revised manuscript for clarity.

For information, the reasons that a CLM4.5 standalone was not included in the original manuscript were:

- (1) The subsurface domain in CLM4.5 for hydrologic processes only extends to 3.8 m below the surface, while in CPv1 subsurface hydrologic processes are simulated ~30m below the surface;
- (2) As reviewed in section 2.2 of the original manuscript, CLM4.5 uses TOPMODEL-based parameterizations to simulate surface and subsurface runoff, as well as mean groundwater table depth using formulations derived from catchment hydrology that do not apply at the field site of interest;
- (3) The key hydrologic progresses (i.e., the exchange of river water and groundwater at the east boundary and lateral transfer of water at all other boundaries) that affect the hydrologic budget of the system are missing from CLM4.5.

*The description of the technical details of the coupling needs more explanation. It is clear that only the soil moisture and hydraulic properties are passed between CLM and PFLOTRAN. However how does this work given that the vertical discretization of CLM differs from PFLOTRAN? The vertical resolution of the subsurface (PFLOTRAN) component is only 0.5*

*meters, while CLM uses layers from mm to m. How does this impact transpiration? Is the default rooting depth used in CLM? How are the 0.5 meter thick layers mapped to the much thinner layers? Does CLM compute freezing and thawing? Which processes are no longer used by CLM in the coupled version?*

**Response:**

In response to all reviewers' comment regarding model coupling, we have significantly revised the technical details about model coupling in Section 2.3 and schematic describing the model coupling in Figure 1 of the revised manuscript.

While the updated section addresses all of the questions raised by the reviewer, we summarize the answers here. The model coupling interface is able to accommodate different vertical and horizontal resolution between the two models. In our present work, both models had the same horizontal resolution, but different vertical resolution. CLM used the default, exponentially varying vertical discretization, but PFLOTRAN had a uniform 0.5 [m] vertical spacing. The vertical extent of the domain in PFLOTRAN is deeper than the CLM domain. The model coupling interface uses conservative interpolation scheme to remap data between two model grids.

Although a study of the changes in computed transpiration due to differences in vertical resolution between CLM and PFLOTRAN is an interesting research investigation, it is beyond the scope of this work. The coupled simulation used the default rooting distribution of CLM. Although PFLOTRAN has a mode that can explicitly handle liquid and ice phase (Karra et al., 2014), in this work, freezing/thaw dynamics was handled by CLM. In this work, CLM's 1D model for flow in unsaturated (Zeng and Decker, 2009) and saturated (Niu et al., 2007) zones are replaced by PFLOTRAN's 3D flow model.

*I am having trouble understanding why the grasses away from the river always have near zero latent heat flux (Figure 7a) while the bare ground has a larger latent heat flux? This explains why the latent heat flux only differs over the bare soil surfaces between CLMPF2m and CLMPFv2m. I fail to understand why the bare soil has a higher latent heat flux than the vegetation, especially given that the moisture available to the roots from horizontal transfer should be even greater than the moisture at the surface. The authors need to explain if this is the expected behavior in CLM, or if it is due to the coupling between PFLOTRAN and CLM.*

**Response:**

It is a known problem that, in CLM4 and CLM4.5, ET could be enhanced when vegetation is removed. This ET enhancement over bare soil has been documented as a counter-intuitive bias for most unsaturated soils in CLM4 and CLM4.5 simulations (Lawrence et al., 2012; Tang and Riley, 2013a). Tang and Riley (2013a) explored a few potential causes for this likely bias (e.g., soil resistance, litter layer resistance, and numerical time step). They found the implementation of a physically based soil resistance lowered the bias slightly, but concluded that the bias remained (Tang and Riley, 2013b). Meanwhile, in studying ET over semiarid regions, Swenson and Lawrence (2014) proposed another soil resistance formulation to fix this excessive soil

evaporation problem within CLM4.5. While their modification improved the simulated terrestrial water storage anomaly and ET when compared to GRACE data and FLUXNET-MTE data, respectively, the empirical nature of the soil resistance proposed could have underestimated the soil resistance variability when compared to other estimates (Tang and Riley, 2013b). Therefore, this is expected behavior in CLM rather than being introduced by the coupling between CLM and PFLOTRAN. We have added discussions in lines 628-642 the revised manuscript.

*Figure 6 should be shown as the difference between the observations and the simulations. This will show much more information concerning how the simulations differ.*

**Response:** We have made changes as suggested. Please check Figure 7 in the revised manuscript for details. We also moved the original figure to the supplementary material as a reference for the readers (i.e., Figure S5).

## References

- Karra, S., Painter, S. L., and Lichtner, P. C.: Three-phase numerical model for subsurface hydrology in permafrost-affected regions (PFLOTRAN-ICE v1.0), *The Cryosphere*, 8, 1935-1950, 10.5194/tc-8-1935-2014, 2014.
- Lawrence, P. J., Feddema, J. J., Bonan, G. B., Meehl, G. A., O'Neill, B. C., Oleson, K. W., Levis, S., Lawrence, D. M., Kluzek, E., Lindsay, K., and Thornton, P. E.: Simulating the Biogeochemical and Biogeophysical Impacts of Transient Land Cover Change and Wood Harvest in the Community Climate System Model (CCSM4) from 1850 to 2100, *Journal of Climate*, 25, 3071-3095, 10.1175/jcli-d-11-00256.1, 2012.
- Niu, G.-Y., Yang, Z.-L., Dickinson, R. E., Gulden, L. E., and Su, H.: Development of a simple groundwater model for use in climate models and evaluation with Gravity Recovery and Climate Experiment data, *Journal of Geophysical Research: Atmospheres*, 112, n/a-n/a, 10.1029/2006JD007522, 2007.
- Swenson, S. C., and Lawrence, D. M.: Assessing a dry surface layer-based soil resistance parameterization for the Community Land Model using GRACE and FLUXNET-MTE data, *Journal of Geophysical Research: Atmospheres*, 119, 20,299-210,312, 10.1002/2014JD022314, 2014.
- Tang, J., and Riley, W. J.: Impacts of a new bare-soil evaporation formulation on site, regional, and global surface energy and water budgets in CLM4, *Journal of Advances in Modeling Earth Systems*, 5, 558-571, 10.1002/jame.20034, 2013a.
- Tang, J. Y., and Riley, W. J.: A new top boundary condition for modeling surface diffusive exchange of a generic volatile tracer: theoretical analysis and application to soil evaporation, *Hydrol. Earth Syst. Sci.*, 17, 873-893, 10.5194/hess-17-873-2013, 2013b.
- Zeng, X., and Decker, M.: Improving the Numerical Solution of Soil Moisture-Based Richards Equation for Land Models with a Deep or Shallow Water Table, *Journal of Hydrometeorology*, 10, 308-319, 10.1175/2008jhm1011.1, 2009.

# **Coupling a three-dimensional subsurface flow and transport model with a land surface model to simulate stream-aquifer-land interactions (CPv1.0) [MS No.: gmd-2017-35]**

## **Responses to review comments**

J. Kala (Editor) j.kala@murdoch.edu.au

*This manuscript is well written. It describes the evaluation and coupling of CLM4.5, a widely used LSM, to PFLOTRAN, a subsurface model. The individual codes and model coupling are well described. The simulations are evaluated under real-life conditions. The paper fits the scope of GMD very well. The paper can be accepted following the following revisions:*

*The most major revision required to this paper is that results with CLM4.5 alone, without coupling to PFLOTRAN, are not presented. The reader hence does not get an idea of the added benefit of running the LSM coupled to a sophisticated subsurface model.*

**Response:** We have added a CLM4.5 standalone simulation for comparison. Please see our response to the referee #1 for more details.

*What are the differences in the surface heat fluxes by running CLM alone versus the coupled system? If sub-surface flows have an influence on the surface energy balance, then it needs to be proved that it is actually worth the effort to run the coupled system?*

**Response:** Please see the response to the question from Referee #1 above. The difference of subsurface flows on surface energy balance is significant between figure S4 (CLM4.5) and Figure 8(a) (i.e., CPv1) in the revised manuscript due to reasons stated in the response to Referee #1.

*The abstract should mention the 3 different spatial resolutions used, especially as it is stated later that spatial resolution had a significant impact. In the abstract, it is also stated that including lateral subsurface flow impacted (I suggest using the word influenced rather than impacted) the surface energy budget and subsurface transport. How?*

**Response:** Thanks for the constructive suggestions. We have added the spatial resolutions to the abstract, changed “impacted” to “influenced”, and added a phrase to discuss the reason why lateral subsurface flow could impact surface energy budget and subsurface transport. Please check the revised abstract for details.

*At the end of the abstract, it is stated that this coupled system could be used to study land-atmosphere interactions. This is not really correct as this current modeling system does not include a dynamic atmospheric component? You ran the model with prescribed meteorology. You cannot really make this conclusion.*

**Response:** Thanks. We have removed that sentence in the revised abstract.

*Line 67 – The acronym ESM does not seem to be have previously defined? Is this acronym really necessary?*

**Response:** Thanks. We have deleted the acronym ESM.

*The introduction gives no indication why coupling CLM and PFLOTRAN is a good and worthwhile idea. Why these two models? If CLM has been coupled to other subsurface models such as PAWS, then what makes PFLOTRAN more advantageous than PAWS? While I have no doubt coupling CLM and PFLOTRAN is a great idea, you need to explain a bit more on why this is the case. Provide a bit more background, one paragraph should do.*

**Response:** In response to this comment and that from the Referee #2, we have added literature reviews and discussions to elaborate the scientific motivation of this study (i.e., the potential of exploring the fully coupled aquifer-soil-vegetation-atmosphere continuum using an integrated model) in Section 1 of the revised manuscript. We also added discussions on how CP v1 differs from CLM-PAWS in lines 115-142 of the revised manuscript as follows:

“The developments of the integrated models have enabled scientific explorations of interactions and feedback mechanisms in the aquifer-soil-vegetation-atmosphere continuum using a holistic and physically based approach (Shrestha et al., 2014; Gilbert et al., 2017). Compared to simulations of regional climate models coupled to traditional LSMs, such a physically based approach shows less sensitivity to uncertainty in the subsurface hydraulic characteristics that could propagate from deep subsurface to free troposphere (Keune et al., 2016), while other physical representations (e.g., parameterizations in evaporation and transpiration, atmospheric boundary layer schemes) could have significant effects on the simulations as well (Sulis et al., 2017). Therefore, it is of great scientific interest to further develop the integrated models and benchmarks to achieve improved understanding of complex interactions in the fully coupled Earth system.

Motivated by the great potentials of using an integrated model to explore Earth system dynamics, the objective of this study is three-fold. First, we aim to document the development of a coupled land surface and subsurface model as a first step toward a new integrated model, featuring the two-way coupling between two highly-scalable and state-of-the-art open-source codes: CLM4.5 [Oleson et al., 2013] and a reactive transport model PFLOTRAN [Lichtner et al., 2015]. The coupled model mechanistically represents the two-way exchange of water and solute mass between aquifers and river, as well as land-atmosphere exchange of water and

energy. The coupled model is therefore named as CP v1.0 hereafter. We note that in recent years, efforts have been made to implement carbon–nitrogen decomposition, nitrification, denitrification, and plant uptake from CLM4.5 in the form of a reaction network solved by PFLOTRAN to enable the coupling of biogeochemical processes between the two models [Tang et al., 2016]. In addition, although PAWS is coupled to the same version of CLM (i.e., CLM4.5) (Ji et al., 2015; Pau et al., 2016), PFLOTRAN resolves the subsurface in a 3-D fashion, while PAWS approximates the 3D Richards equation by divide the subsurface into an unsaturated domain represented by the 1-D Richards Equation coupled with 3D saturated groundwater flow equation for subsurface flow, by assuming that there is no horizontal flow in unsaturated portion of soil, and that lateral flux in saturated portion is evenly distributed.”

*The paper tends to make use of many acronyms, and many of these do not seem necessary. Please only use acronyms where it is warranted. For example, the LEAF acronym is only used once, so there is no point in defining it if you don't use it again. Please carefully review all your acronyms.*

**Response:** Thanks. We have deleted all unnecessary acronyms.

*In Figure 1, some of the arrows do not seem to make sense to me. CLM links directly to PFLOTRAN Initialize, execute and finalize. Surely, CLM should only link to PLFOTRAN initialize, when then links to PFLOTRAN execute, then finalize. Also, according to your diagram, no information flows back from PFLOTRAN to CLM? Your diagram suggests that there is no two-way coupling? But the text state that soil moisture and hydraulic properties from PFLOTRAN and given back to CLM. Your flowchart does not really show this? Use m day-1 rather than m d-1.*

**Response:** In response to all reviewers' comment regarding model coupling, we have significantly revised the technical details about model coupling in Section 2.3 (see below as well) and added a new schematic describing the model coupling (Figure 1) in the revised manuscript. We have updated Figure 1 to better represent the two-way model coupling. We also have changed the unit “m d-1” to “m day-1”.

While the updated section addresses all of the questions raised by the reviewer, we summarize the answers here. The model coupling interface is able to accommodate different vertical and horizontal resolution between the two models. In our present work, both models had the same horizontal resolution, but different vertical resolution. CLM used the default, exponentially varying vertical discretization, but PFLOTRAN had a uniform 0.5 [m] vertical spacing. The vertical extent of the domain in PFLOTRAN is deeper than the CLM domain. The model coupling interface uses conservative interpolation scheme to remap data between two model grids.

*Figure 4 – Sorry I can hardly read any of the figure titles, please make these larger and more easily readable.*

**Response:** Thanks for pointing this out. We have made the font of the figure titles bigger in the revised manuscript, including those in supplementary materials (figures S1 and S2).

*Lines 359 – 361: You state that cold month were excluded from the analysis as you end up with division by zero issues when LH becomes close to zero. That’s why most people use the evaporative fraction (EF), rather than the Bowen ratio. With EF, you take the ratio of latent to the sum of sensible and latent, hence, you will not have division by zero issues. You should use EF rather than Bowen ratio.*

**Response:** Thanks for the great suggestion. We have redone the analysis using EF instead of Bowen ratio, and modified the figure and text in the revised manuscript correspondingly.

*Section 4.1 – Please use model evaluation rather than model validation. Validation implies the model is already correct to start with and you are therefore validating it. This is of course never true of any model.*

**Response:** Thanks for the great suggestion. We have changed the section title to be “Model evaluation”.

*Line 418: Looking at Figure 7(a) and 8, I find it hard to get an accurate idea of the differences, could you please plot the difference instead? Figure 10 – can you please remove the textbox at the bottom (CONTOUR FROM.....). Looks like an NCL plot to me  
I’m sure you can remove this: `ares@cnInfoLabelOn = False`*

**Response:** We have modified the figures as suggested. Please check the revised manuscript for details. We also modified the figures in the supplementary material accordingly to be consistent.

*Line 447: Don’t start a sentence with And. Your use of the 2 m simulation as a surrogate truth is fine, given a lack of observations of what is being simulated. However, you cannot really say simulation x outperformed simulation y (line 482), explain why one simulation appears more realistic, but I am not comfortable with the word “outperform”. It would have been really interesting if you ran your model over a site for which observationally derived flux tower estimates of H and LE are available, such that you could then assess if this coupled system actually improves on CLM4.5 alone in simulating surface energy fluxes. I do understand that locations where Flux tower data are currently available (e.g., the FLUXNET network), may not necessarily be regions where the hydrology is interesting enough to warrant the use of such a model. You do however, need to acknowledge somewhere that the model needs to be evaluated against actual observations of surface fluxes.*

**Response:** Thanks for the great suggestions. We have modified the sentences as suggested in the revised manuscript. In fact, two flux towers have been installed along the Hanford reach for this purpose but the analysis of the flux measurement is still preliminary. In addition, both towers are a little distant from the modeling domain to satisfy the requirements of eddy covariance measurements. Nevertheless, we also added discussions on the need of evaluating the model using eddy covariance measurements in lines 622-627 of the revised manuscript.

*Code availability: We had a recent discussion among GMD editors, and the point of the Code Availability section is to ensure the reproducibility. What we want is the exact code used for this paper. It is of course understandable that the code is still under development, however, we request you make the version of the code used for this paper available. If this is already on bitbucket or github, it is quite easy to make the revision/branch used for this study on ZENODO, which is the preferred repository for code as per GMD guidelines as it will generate an actual DOI for the code: [http://www.geoscientific-model-development.net/about/code\\_and\\_data\\_policy.html](http://www.geoscientific-model-development.net/about/code_and_data_policy.html)*

*If you do a quick search on ZENODO, you will find several codes which point to github/bitbucket repositories, but a “frozen” version of the code used can be directly obtained from ZENODO, rather than a user having to work out which branch/revision of your code was used in the paper from the github/bitbucket repo*

**Response:** Thanks for the instruction. The model and data have been made publicly available at

- [https://bitbucket.org/clm\\_pflotran/clm-pflotran-trunk](https://bitbucket.org/clm_pflotran/clm-pflotran-trunk): CLM code
- [https://bitbucket.org/clm\\_pflotran/pflotran-clm-trunk](https://bitbucket.org/clm_pflotran/pflotran-clm-trunk): PFLOTRAN code
- [https://bitbucket.org/pnnl\\_sbr\\_sfa/notes-for-gmd-2017-35](https://bitbucket.org/pnnl_sbr_sfa/notes-for-gmd-2017-35): Data

The README file in the notes-for-gmd-2017-35 repository provides detailed notes on how to create, compile, and run a simulation. This information has been incorporated into the “code availability” section of the revised manuscript. Once the manuscript is accepted, we will start porting the frozen version of the code to ZENODO.

## Reference:

Gilbert, J. M., Maxwell, R. M., and Gochis, D. J.: Effects of Water-Table Configuration on the Planetary Boundary Layer over the San Joaquin River Watershed, California, *Journal of Hydrometeorology*, 18, 1471-1488, 10.1175/jhm-d-16-0134.1, 2017.

Hammond, G. E., and Lichtner, P. C.: Field-scale model for the natural attenuation of uranium at the Hanford 300 Area using high-performance computing, *Water Resources Research*, 46, n/a-n/a, 10.1029/2009WR008819, 2010.

Ji, X., Shen, C., and Riley, W. J.: Temporal evolution of soil moisture statistical fractal and controls by soil texture and regional groundwater flow, *Advances in Water Resources*, 86, Part A, 155-169, <http://dx.doi.org/10.1016/j.advwatres.2015.09.027>, 2015.

Karra, S., Painter, S. L., and Lichtner, P. C.: Three-phase numerical model for subsurface hydrology in permafrost-affected regions (PFLOTRAN-ICE v1.0), *The Cryosphere*, 8, 1935-1950, 10.5194/tc-8-1935-2014, 2014.

Keune, J., Gasper, F., Goergen, K., Hense, A., Shrestha, P., Sulis, M., and Kollet, S.: Studying the influence of groundwater representations on land surface-atmosphere feedbacks during the European heat wave in 2003, *Journal of Geophysical Research: Atmospheres*, 121, 301-313, 10.1002/2016JD025426, 2016.

Niu, G.-Y., Yang, Z.-L., Dickinson, R. E., Gulden, L. E., and Su, H.: Development of a simple groundwater model for use in climate models and evaluation with Gravity Recovery and Climate Experiment data, *Journal of Geophysical Research: Atmospheres*, 112, n/a-n/a, 10.1029/2006JD007522, 2007.

Pau, G. S. H., Shen, C., Riley, W. J., and Liu, Y.: Accurate and efficient prediction of fine-resolution hydrologic and carbon dynamic simulations from coarse-resolution models, *Water Resources Research*, 52, 791-812, 10.1002/2015WR017782, 2016.

Shrestha, P., Sulis, M., Masbou, M., Kollet, S., and Simmer, C.: A Scale-Consistent Terrestrial Systems Modeling Platform Based on COSMO, CLM, and ParFlow, *Monthly Weather Review*, 142, 3466-3483, 10.1175/mwr-d-14-00029.1, 2014.

Sulis, M., Williams, J. L., Shrestha, P., Diederich, M., Simmer, C., Kollet, S. J., and Maxwell, R. M.: Coupling Groundwater, Vegetation, and Atmospheric Processes: A Comparison of Two Integrated Models, *Journal of Hydrometeorology*, 18, 1489-1511, 10.1175/jhm-d-16-0159.1, 2017.

Tang, G., Yuan, F., Bisht, G., Hammond, G. E., Lichtner, P. C., Kumar, J., Mills, R. T., Xu, X., Andre, B., Hoffman, F. M., Painter, S. L., and Thornton, P. E.: Addressing numerical challenges in introducing a reactive transport code into a land surface model: a biogeochemical modeling proof-of-concept with CLM-PFLOTRAN 1.0, *Geosci. Model Dev.*, 9, 927-946, 10.5194/gmd-9-927-2016, 2016.

Zachara, J. M., Chen, X., Murray, C., and Hammond, G.: River stage influences on uranium transport in a hydrologically dynamic groundwater-surface water transition zone, *Water Resources Research*, 52, 1568-1590, 10.1002/2015WR018009, 2016.

Zeng, X., and Decker, M.: Improving the Numerical Solution of Soil Moisture-Based Richards Equation for Land Models with a Deep or Shallow Water Table, *Journal of Hydrometeorology*, 10, 308-319, 10.1175/2008JHM1011.1, 2009.

# **Coupling a three-dimensional subsurface flow and transport model with a land surface model to simulate stream-aquifer-land interactions (CPv1.0) [MS No.: gmd-2017-35]**

## **Responses to review comments**

### **Anonymous Referee #2**

*In this manuscript the authors document development and application of a coupled Richards' equation solver (PFLOTRAN) with a land surface model (CLM 4.5) and apply it to a test problem developed from an intensely observed floodplain system. This manuscript is generally clearly written but in my opinion needs to better articulate its contributions given the prior work on this topic. I have specific comments below that need to be addressed before the suitability of this work for GMD can be assessed.*

*The larger comments are ones of contribution, what does this work want to contribute to our understanding of coupling models? Given that the main contribution (as I see it) is the coupler yet this is not novel i think the authors have the challenge to clearly articulate what their contribution is. I encourage them to revise their manuscript accordingly to do this.*

*1. Introduction. The background provided in the introduction is a nice overview.*

**Response:** Thanks for the positive comments.

*2. Lines 91-97, the authors should also include TerrSysMP system (Shrestha et al MWR 2104) in this list and perhaps the numerous follow up studies using this platform. The platform is particularly important as it couples the same LSM as used in this study (CLM 3.5, now 4.5) coupled to an integrated hydrology model. As examples, the authors of this platform have used it for fully-coupled studies over all of Europe (Keune et al. JGR-A 2016) and for high resolution simulation (Gebler et al JoH 2017). It strikes me that these studies are much more advanced than the current effort and should be used to demonstrate how the current study is advancing the science.*

**Response:** Thanks for the great suggestion. We have added reviews on these studies in the introduction section of the revised manuscripts, and added discussions on how such coupled models could advance science in lines 115-125 of the revised manuscript as follows:

“The developments of the integrated models have enabled scientific explorations of interactions and feedback mechanisms in the aquifer-soil-vegetation-atmosphere continuum using a holistic and physically based approach (Shrestha et al., 2014; Gilbert et al., 2017). Compared to simulations of regional climate models coupled to traditional LSMs, such a physically based approach shows less sensitivity to uncertainty in the subsurface hydraulic

characteristics that could propagate from deep subsurface to free troposphere (Keune et al., 2016), while other physical representations (e.g., parameterizations in evaporation and transpiration, atmospheric boundary layer schemes) could have significant effects on the simulations as well (Sulis et al., 2017). Therefore, it is of great scientific interest to further develop the integrated models and benchmarks to achieve improved understanding of complex interactions in the fully coupled Earth system.”

3. *Lines 103-104, the sentence is confusing. Do you mean that sometimes models agree and sometimes they don't?*

**Response:** Thanks for pointing this out. We have modified this sentence as follows in lines 107-114 of the revised manuscript:

“However, as a result of difference in physical process representations and numerical solution approaches in terms of (1) the coupling between the variably saturated groundwater and surface water flow; (2) representation of surface water flow; and (3) implementation of subsurface heterogeneity in the existing integrated models, significant discrepancies exist in their results when the models were applied to highly nonlinear problems with heterogeneity and complex water table dynamics, while many of the models show good agreement for simpler test cases where traditional runoff generation mechanisms (i.e., saturation and infiltration excess runoff) apply (Kollet et al., 2017; Maxwell et al., 2014).”

4. *Paragraph starting at line 107. This paragraph should be re-structured. One of the main criticisms I have of this work is the lack of novelty. This paragraph is one of the main places the authors can distinguish their work from prior studies. They don't in fact show scalability of either code and the other two points are somewhat weak science goals. I think restructuring this paragraph will help the authors develop a manuscript that is better organized and articulates the contributions made by this work.*

**Response:** Thanks for the constructive comments. We have revised this section significantly to include discussions on the scientific potential of integrated models based on recent studies. We also revised the coupling section to provide more details on how the coupling was achieved. Please check section 1 of the revised manuscript to see if the revisions are satisfactory.

5. *Integrated hydrology models are such (and not just Richards' solvers) because they solve a form of the shallow water equations and Richards' equation in a globally implicit manner. It is unclear that PFLOTRAN has a surface component, so is it an integrated code?*

**Response:** In this study, a prognostic model for simulating river stage dynamics is not included. Instead, a river stage boundary condition was applied to PFLOTRAN to capture observed and hypothetical river stage scenarios. Even though a shallow water equation implementation in PFLOTRAN is under testing, it is premature and warrants a standalone study to assess its performance. Therefore, we have modified the text throughout the revised manuscript to remove ambiguity in this regard. We also added the need of implementing a surface flow component to

qualify the model as an integrated hydrology model into the discussion section. Please check the revised manuscript for detail.

6. *Lines 205-220. As I see it, the coupler is the only potential contribution made in this work. The description needs to be much more detailed. What fluxes and states are passed between the two codes? How is the gridding handled? How is the parallelization accomplished for tiling in CLM and cells in PFLOTRAN? How is the grid overlap between soil column and 3D mesh approached, is the 3D Richards' formulation used in place of CLM or is there some other point where the codes couple? What time integration strategy is used? These are all critical points that should be addressed.*

**Response:** In response to all reviewers' comment regarding model coupling, we have significantly revised the technical details about model coupling in Section 2.3 and added a new schematic (Figure 1) to describe the two-way model coupling in the revised manuscript. We attempted to answer all the specific questions of this comment. The models are coupled two-ways and we have updated Figure 1 to better represent model coupling as follows. Please section 2.3 of the revised manuscript for detailed description on this coupling.

7. *Lines 218-220. Surely the authors don't mean this is the first study to couple 3D Richards' equation to a land surface model, that has been documented in the literature for more than a decade. Do the authors mean the PFLOTRAN CLM 4.5 coupling? That isn't novel. This sentence makes the authors sound either disingenuous or naive, either way I think it should be restructured or removed.*

**Response:** Thanks for the suggestion. We have deleted this sentence.

8. *Verification. There is no section describing the verification of the modeling approach. Prior studies have carefully calculated the energy and water balance of the individual and coupled systems to ensure that nothing in the original formulations has been altered by the coupling and that the coupled system balances water and energy between models. This is a critical missing aspect of the work. It's important to distinguish this from model validation, where a system that is poorly constructed could still be tuned to match observations.*

**Response:** We agree that a thorough evaluation of the energy and water balance terms is needed for the system. To address the reviewer's concern, we have (1) verified that the subsurface solver by evaluating the mass balance errors for each time step and added the figure to the supplementary material; and (2) verified that the surface energy balance and added the figure to the supplementary material. Discussions on these figures were added in lines 441-444 of the revised manuscript.

9. *PFCLM. The abbreviation PFCLM has been used widely in the literature for the coupled codes ParFlow and CLM. The use here is confusing and a different acronym should be chosen.*

Also, given the order of calling (PFLOTRAN is a subroutine of CLM 4.5) it seems the CLM component leads, not the hydrology one.

**Response:** Thanks for the constructive suggestion. We have changed the model name to be CP v1.0 to be consistent with the sequence of coupling, and to differentiate the model from ParFlow-CLM and previous coupled versions of CLM4.5 and PFLOTRAN. We have modified all occurrences of the names in the text and figures. Please check the revised manuscripts for details.

*10. Scale. The Hanford test case appears to be at very fine spatial resolution (2m) which violates most of the assumptions made for land-energy fluxes in CLM. The M-O stability and ET formulations use a single-column approach which would almost assuredly break down at this resolution. Studies that do consider this type of fine scale usually use LES formulations for the atmosphere to relax this assumption. The authors need to discuss this and perhaps discard the 2m case.*

**Response:** As noted by the reviewer, CLM uses the M-O similarity theory to compute friction velocity and other exchange coefficients that provide the basis to estimate surface heat and moisture fluxes. It is also common knowledge that the M-O similarity theory is only valid when the surface layer depth  $z \gg z_0$ , where  $z_0$  is the aerodynamic roughness length. As reviewed in Basu and Lacser (2017), It is highly recommended that  $z > 50z_0$  to ensure that the lower atmospheric level is higher than the size of surface wakes in the roughness sublayer, which should be proportional to horizontal grid spacing to guarantee the validity of the M-O similarity theory (Arnqvist and Bergström, 2015).

In our simulations, the majority of the Hanford 300A domain is covered by bare soil ( $z_0 = 0.01$  m), grass ( $z_0 = 0.013$  m), shrubs ( $z_0 = 0.026-0.043$  m), and riparian trees (varies across the seasons,  $z_0 = 0.008$  m when LAI = 2 in the summer and  $z_0 = 1.4$  when LAI = 0 in the winter). Therefore, under most condition a 2-m resolution is sufficiently coarse to ensure the validity of the M-O similarity theory, except for the grid cells covered by riparian trees in the winter. However, in our simulations, the wintertime latent heat and sensible heat fluxes approach zero due to extremely low energy inputs in the winter. In addition, the 2-m resolution simulations are valuable for verifying subsurface simulations. Therefore, after careful considerations, we decide to keep the 2-m simulations, but added discussion on potential issues when the model is run at such a resolution in lines 608-621 of section 5 in the revised manuscript. We hope such a treatment could alleviate problems associated with the scale of model applicability.

## Reference:

- Arnqvist, J., and Bergström, H.: Flux-profile relation with roughness sublayer correction, *Quarterly Journal of the Royal Meteorological Society*, 141, 1191-1197, 10.1002/qj.2426, 2015.
- Basu, S., and Lacser, A.: A Cautionary Note on the Use of Monin–Obukhov Similarity Theory in Very High-Resolution Large-Eddy Simulations, *Boundary-Layer Meteorology*, 163, 351-355, 10.1007/s10546-016-0225-y, 2017.
- Gilbert, J. M., Maxwell, R. M., and Gochis, D. J.: Effects of Water-Table Configuration on the Planetary Boundary Layer over the San Joaquin River Watershed, California, *Journal of Hydrometeorology*, 18, 1471-1488, 10.1175/jhm-d-16-0134.1, 2017.
- Keune, J., Gasper, F., Goergen, K., Hense, A., Shrestha, P., Sulis, M., and Kollet, S.: Studying the influence of groundwater representations on land surface-atmosphere feedbacks during the European heat wave in 2003, *Journal of Geophysical Research: Atmospheres*, 121, 301-313, 325, 10.1002/2016JD025426, 2016.
- Kollet, S., Sulis, M., Maxwell, R. M., Paniconi, C., Putti, M., Bertoldi, G., Coon, E. T., Cordano, E., Endrizzi, S., Kikinzon, E., Mouche, E., Mügler, C., Park, Y.-J., Refsgaard, J. C., Stisen, S., and Sudicky, E.: The integrated hydrologic model intercomparison project, IH-MIP2: A second set of benchmark results to diagnose integrated hydrology and feedbacks, *Water Resources Research*, 53, 867-890, 10.1002/2016WR019191, 2017.
- Maxwell, R. M., Putti, M., Meyerhoff, S., Delfs, J.-O., Ferguson, I. M., Ivanov, V., Kim, J., Kolditz, O., Kollet, S. J., Kumar, M., Lopez, S., Niu, J., Paniconi, C., Park, Y.-J., Phanikumar, M. S., Shen, C., Sudicky, E. A., and Sulis, M.: Surface-subsurface model intercomparison: A first set of benchmark results to diagnose integrated hydrology and feedbacks, *Water Resources Research*, 50, 1531-1549, 10.1002/2013WR013725, 2014.
- Shrestha, P., Sulis, M., Masbou, M., Kollet, S., and Simmer, C.: A Scale-Consistent Terrestrial Systems Modeling Platform Based on COSMO, CLM, and ParFlow, *Monthly Weather Review*, 142, 3466-3483, 10.1175/mwr-d-14-00029.1, 2014.
- Sulis, M., Williams, J. L., Shrestha, P., Diederich, M., Simmer, C., Kollet, S. J., and Maxwell, R. M.: Coupling Groundwater, Vegetation, and Atmospheric Processes: A Comparison of Two Integrated Models, *Journal of Hydrometeorology*, 18, 1489-1511, 10.1175/jhm-d-16-0159.1, 2017.

# Coupling a three-dimensional subsurface flow and transport model with a land surface model to simulate stream-aquifer-land interactions ([PFLOTRAN\\_CLM\\_CP](#) v1.0)

Gautam Bisht<sup>1</sup>, Maoyi Huang<sup>2,\*</sup>, Tian Zhou<sup>2</sup>, Xingyuan Chen<sup>2</sup>, Heng Dai<sup>2</sup>, Glenn Hammond<sup>3</sup>, William Riley<sup>1</sup>, Janelle Downs<sup>2</sup>, Ying Liu<sup>2</sup>, John Zachara<sup>2</sup>

<sup>1</sup>Lawrence Berkeley National Laboratory, Berkeley, CA

<sup>2</sup>Pacific Northwest National Laboratory, Richland, WA

<sup>3</sup>Sandia National Laboratories, Albuquerque, NM

Correspondence to: Maoyi Huang (maoyi.huang@pnnl.gov)

[Revised](#) Manuscript to be considered for *Geoscientific Model Development*

## Abstract

A fully coupled three-dimensional surface and subsurface land model is developed and applied to a site along the Columbia River to simulate three-way interactions among river water, groundwater, and land surface processes. The model features the coupling of the Community Land Model version 4.5 (CLM4.5) and a massively-parallel multi-physics reactive transport model (PFLOTRAN). The coupled model, named [PFLOTRAN-CLM-PFLOTRAN-SIZCP](#) v1.0, is applied to a 400 m × 400 m study domain instrumented with groundwater monitoring wells along the Columbia River shoreline. [PFLOTRAN-CLM-PFLOTRAN-SIZCP](#) v1.0 simulations are performed at three spatial resolutions (*i.e.*, 2 m, 10 m, and 20 m) over a five-year period to evaluate the impact of hydro-climatic conditions and spatial resolution on simulated variables. Results show that the coupled model is capable of simulating groundwater-river water interactions driven by river stage variability along managed river reaches, which are of global significance as a result of over 30,000 dams constructed worldwide during the past half century. Our numerical experiments suggest that the land-surface energy partitioning is strongly modulated by groundwater-river water interactions through expanding the periodically inundated fraction of the riparian zone, and enhancing moisture availability in the vadose zone via capillary rise in response to the river stage change. Furthermore, spatial resolution is found to impact significantly the accuracy of estimated the mass exchange rates at the boundaries of the aquifer, and it becomes critical when surface and subsurface become more tightly coupled with groundwater table within six to seven meters below the surface. Inclusion of lateral subsurface flow [impacted-influenced](#) both the surface energy budget and subsurface transport processes [as a result of river water intrusion into the subsurface in response to elevated river stage that increased soil moisture for evapotranspiration and suppressed available energy for sensible heat in the warm season.](#) The coupled model developed in this study can be used for improving mechanistic understanding of ecosystem functioning ~~,-and~~ biogeochemical cycling ~~,and land-atmosphere interactions~~ along river corridors under historical and future hydro-climatic changes. The dataset presented in this study can also serve as a good benchmarking case for testing other integrated models.

## 1 Introduction

Previous modeling studies have demonstrated that subsurface hydrologic model structure and parameterization can significantly affect simulated land-atmosphere exchanges [Condon *et al.*, 2013; Hou *et al.*, 2012; Kollet and Maxwell, 2008; Miguez-Macho and Fan, 2012] and therefore boundary layer dynamics [Maxwell and Miller, 2005; Rihani *et al.*, 2015], cloud formation [Rahman *et al.*, 2015], and climate [Leung *et al.*, 2011; Taylor *et al.*, 2013]. Lateral subsurface processes are fundamentally important at multiple spatial scales, including hill-slope scales [McNamara *et al.*, 2005; Zhang *et al.*, 2011], basin scales in semi-arid and arid climates where regional aquifers sustain baseflows in rivers [Schaller and Fan, 2009], and wetlands [Fan and Miguez-Macho, 2011]. However, some ~~current-current-generation of~~ land surface models (LSMs) routinely omit explicit lateral subsurface processes [Clark *et al.*, 2015; Kollet and Maxwell, 2008; Nir *et al.*, 2014], while others include them (described below). Observational and modeling studies suggest that groundwater forms an environmental gradient in soil moisture availability by redistributing water that could profoundly shape critical zone evolution at continental to global scales [Fan *et al.*, 2013; Taylor *et al.*, 2013]. The mismatch between observed and simulated evapotranspiration by current LSMs could be explained by the absence of lateral groundwater flow [Maxwell and Condon, 2016].

It has been increasingly recognized that rivers, despite their small aerial extent on the landscape, play important roles in watershed functioning through their connections with groundwater aquifers and riparian zones [Shen *et al.*, 2016]. The interactions between groundwater and river water prolong physical storage and enhance reactive processing that alter water chemistry, downstream transport of materials and energy, and biogenic gas emissions [Fischer *et al.*, 2005; Harvey and Gooseff, 2015]. The Earth System modeling community recognizes such a gap in existing ~~Earth system models SMs~~ and calls for improved representation of biophysical and biogeochemical processes within the terrestrial-aquatic interface [Gaillardet *et al.*, 2014].

Over the past decade, much effort has been expended to include groundwater into LSMs. Groundwater is important to water and energy budgets such as evapotranspiration (ET), latent heat (LH), and sensible heat (SH), but also to biogeochemical processes such as gross primary production (~~GPP~~), heterotrophic respiration (~~HR~~), and nutrient cycling. The lateral convergence of water along the landscape and two-way groundwater-surface water exchange are identified as

the most relevant subsurface processes to large-scale Earth System functioning (see review by *Clark et al.* [2015]). However, the choice of processes, the approaches to represent multi-scale structures and heterogeneities, the data and computational demands, etc., all vary greatly among the research groups even working on the same land models.

Most of the LSMs reviewed by *Clark et al.* [2015] do not explicitly account for stream-aquifer-land interactions. For example, the Community Land Model version 4.5 allows for re-infiltration of flooded waters in a highly parameterized way without explicitly linking to groundwater dynamics, therefore only one-way flow from the aquifer to the stream is simulated [*Oleson et al.*, 2013]. The Land-Ecosystem-Atmosphere Feedback (~~LEAF~~)-model treats river elevation as part of the 2-D vertically integrated groundwater flow equation and allows river and floodwater to infiltrate through sediments in the flood plain [*Miguez-Macho and Fan*, 2012].

In contrast, the fully integrated models, being a small subset of LSMs, explicitly represent the two-way exchange between groundwater aquifers and their adjacent rivers in a spatially resolved fashion. Such models couple a completely integrated hydrology model with a land surface model, so that the surface-water recharge to groundwater by infiltration or intrusion and base flow discharge from groundwater to surface waters can be estimated in a more mechanistic way.

Examples of the ~~fully~~-integrated models include: (1) the coupling between the Common Land Model (CoLM) and a variably saturated groundwater model (ParFlow) [*Maxwell and Miller*, 2005]; (2) the Penn State Integrated Hydrologic Model (PIHM) [*Shi et al.*, 2013]; (3) the coupling between the Process-based Adaptive Watershed Simulator (PAWS) and CLM4.5 [*Ji et al.*, 2015; *Pau et al.*, 2016; *Riley and Shen*, 2014]; ~~and~~ (4) the coupling between the CATchment Hydrology (CATHY) model and the Noah model with multiple parameterization schemes (Noah-MP) [*Niu et al.*, 2014]; and (5) the coupling between CLM3.5 and ParFlow through the Ocean Atmosphere Sea Ice Soil external coupler (OASIS3) in the Terrestrial Systems Modeling Platform (TerrSysMP) [*Shrestha et al.*, 2014; *Gebler et al.*, 2017]. The integrated models eliminate the need for parameterizing lateral groundwater flow and allow the interconnected groundwater-surface-water systems to evolve dynamically based on the governing equations and the properties of the physical system. Although such models often require robust numerical solvers on high-performance computing (HPC) facilities to achieve high-resolution, large-extent simulations [*Maxwell et al.*, 2015], they have been increasingly applied for hydrologic prediction

and environmental understanding. However, as a result of difference in physical process representations and numerical solution approaches in terms of (1) the coupling between the variably saturated groundwater and surface water flow; (2) representation of surface water flow; and (3) implementation of subsurface heterogeneity in the existing integrated models, significant discrepancies exist in their simulations results when the models were being applied to complex highly nonlinear problems with heterogeneity and complex water table dynamics due to differences in physical process representations and numerical solution approaches, even though while many of the models show good agreement for simpler test cases where traditional runoff generation mechanisms (i.e., saturation and infiltration excess runoff) apply [Kollet et al., 2017; Maxwell et al., 2014].

We have three aims in this paper. The developments of the integrated models have enabled scientific explorations of interactions and feedback mechanisms in the aquifer-soil-vegetation-atmosphere continuum using a holistic and physically based approach [Shrestha et al., 2014; Gilbert et al., 2017]. Compared to simulations of regional climate models coupled to traditional LSMs, such a physically based approach shows less sensitivity to uncertainty in the subsurface hydraulic characteristics that could propagate from deep subsurface to free troposphere [Keune et al., 2016], while other physical representations (e.g., parameterizations in evaporation and transpiration, atmospheric boundary layer schemes) could have significant effects on the simulations as well [Sulis et al., 2017]. Therefore, it is of great scientific interest to further develop the integrated models and benchmarks to achieve improved understanding of complex interactions in the fully coupled Earth system.

Motivated by the great potentials of using an integrated model to explore Earth system dynamics, the objective of this study is three-fold. First, we aim to document the development of a fully integrated-coupled land surface and subsurface model as a first step toward a new integrated model, featuring the two-way coupling between two highly-scalable and state-of-the-art open-source codes: CLM4.5 [Oleson et al., 2013] and a reactive transport model PFLOTRAN [Lichtner et al., 2015] and CLM4.5 [Oleson et al., 2013] (PFLOTRAN-CLM v1.0 hereafter). The coupled model that mechanistically represents the two-way exchange of water and solute mass between aquifers and river, as well as land-atmosphere exchange of water and energy. The coupled model is therefore named as CLM-PFLOTRAN-SIZCP v1.0 hereafter. We note that in recent years, efforts have been made to implement carbon-nitrogen decomposition, nitrification,

denitrification, and plant uptake from CLM4.5 in the form of a reaction network solved by PFLOTRAN to enable the coupling of biogeochemical processes between the two models [Tang et al., 2016]. In addition, although PAWS is coupled to the same version of CLM (i.e., CLM4.5) [Ji et al., 2015; Pau et al., 2016], PFLOTRAN resolves the subsurface in a 3-D fashion, while PAWS approximates the 3D Richards equation by divide the subsurface into an unsaturated domain represented by the 1-D Richards Equation coupled with 3D saturated groundwater flow equation for subsurface flow, by assuming that there is no horizontal flow in unsaturated portion of soil, and that lateral flux in saturated portion is evenly distributed.

Second, we describe a numerically challenging benchmarking case for verifying ~~fully integrated-coupled land surface and subsurface~~ models, featuring a highly dynamic river boundary condition determined by dam-induced river stage variations (Hauer et al., 2017), representative of managed river reaches that are of global significance as a result of dam constructions in the past few decades [Zhou et al., 2016]. Third, we assess the effects of spatial resolution and projected hydro-climatic changes on simulated land surface fluxes and exchange of groundwater and river water using the coupled model and datasets from the benchmarking case. In section 2, we describe the component models and our coupling strategy. In section 3, we describe an application of the model to a field site along the Hanford reach of the Columbia River, where the subsurface properties are well characterized and long-term monitoring of river stage, groundwater table, and exchange of groundwater and river water exist. In section 4, we assess the effects of spatial resolution and hydro-climatic conditions to simulated fluxes and state variables. In section 5, conclusion and future work are discussed.

## **2 Model description**

### **2.1 The Community Land Model version 4.5**

CLM4.5 [Oleson et al., 2013] is the land component of the Community Earth System Model version 1 (CESM1) [Hurrell et al., 2013], a fully coupled numerical simulator of the Earth system consisting of atmospheric, ocean, ice, land surface, carbon cycle, and other components (~~top panel of Figure 1~~). It has been applied successfully to explore interactions among water, energy, carbon, and biogeochemical cycling at local to global scales [Leng et al., 2016b; Xu et al., 2016], and proven to be highly scalable on leading HPC facilities such as the U.S.

Department of Energy (USDOE)'s National Energy Research Scientific Computing Center (NERSC). The model includes parameterizations of terrestrial hydrological processes including interception, throughfall, canopy drip, snow accumulation and melt, water transfer between snow layers, infiltration, evaporation, surface runoff, sub-surface drainage, redistribution within the soil column, and groundwater discharge and recharge to simulate changes in canopy water, surface water, snow water, soil water, and soil ice, and water in the unconfined aquifer [Oleson *et al.*, 2013]. Precipitation is either intercepted by the canopy, falls directly to the snow/soil surface (throughfall), or drips off the vegetation (canopy drip). Water input at the land surface, the sum of liquid precipitation reaching the ground and melt water from snow, is partitioned into surface runoff, surface water storage, and infiltration into the soil. Two sets of runoff generation parameterizations, including formulations for saturation and infiltration excess runoff and baseflow, are implemented into the model: the TOPMODEL-based runoff generation formulations [Beven and Kirkby, 1979; Niu *et al.*, 2005; Niu *et al.*, 2007] and the Variable Infiltration Capacity (VIC)-based runoff generation formulations [Lei *et al.*, 2014; Liang *et al.*, 1994; Wood *et al.*, 1992]. Surface water storage and outflow in and from wetlands and small sub-grid scale water bodies are parameterized as functions of fine-spatial-scale elevation variations called microtopography. Soil water is predicted from a multi-layer model based on the 1-D Richards equation, with boundary conditions and source/sink terms specified as infiltration, surface and sub-surface runoff, gradient diffusion, gravity, canopy transpiration through root extraction, and interactions with groundwater. A groundwater component is added in the form of an unconfined aquifer lying below the soil column following Niu *et al.* [2007]. [The model computes Zeng et al. \(1998\) surface energy fluxes following the Monin-Obukhov Similarity Theory using formulations in Zeng et al. \(1998\), with which updates the calculation of boundary resistance terms calculated based on updated formulations to account for understory turbulence, sparse and dense canopies, and surface litter layer](#) (Sakaguchi and Zeng, 2009; Zeng *et al.*, 2005; Zeng and Wang, 2007). [Water and energy budgets are conserved at every modeling step.](#)

## 2.2 PFLOTRAN

PFLOTRAN is a massively-parallel multi-physics simulator [Hammond *et al.*, 2014] developed and distributed under an open source GNU LGPL license and is freely available through Bitbucket (<https://bitbucket.org/pflotran/pflotran>)~~<https://bitbucket.org/pflotran/pflotran-dev>~~. It

solves a system of generally nonlinear partial differential equations (PDEs) describing multiphase, multicomponent and multiscale reactive flow and transport in porous materials. The PDEs are spatially discretized using a finite volume technique, and the backward Euler scheme is used for implicit time discretization. It has been widely used for simulating subsurface multiphase flow and reactive biogeochemical transport processes [*Chen et al.*, 2013; *Chen et al.*, 2012; *Hammond and Lichtner*, 2010; *Hammond et al.*, 2011; *Kumar et al.*, 2016; *Lichtner and Hammond*, 2012; *Liu et al.*, 2016; *Pau et al.*, 2014]

PFLOTRAN is written in object-oriented Fortran 2003/2008 and relies on the PETSc framework [*Balay et al.*, 2015] to provide the underlying parallel data structures and solvers for scalable high performance computing. PFLOTRAN uses domain decomposition and MPI libraries for parallelization. PFLOTRAN has been run on problems composed of over 3 billion degrees of freedom with up to 262,144 processors, but it is more commonly employed on problems with millions to tens of millions of degrees of freedom utilizing hundreds to thousands of processors. Although PFLOTRAN is designed for massively parallel computation, the same code base can be run on a single processor without recompiling, which may limit problem size based on available memory.

In this study, PFLOTRAN is used to simulate single phase variably saturated flow and solute transport in the subsurface. Single-phase variably saturated flow is based on the Richards equation with the form

$$\frac{\partial}{\partial t}(\varphi s \rho) + \nabla \cdot \rho \mathbf{q} = 0, \quad (1)$$

with [waterliquid](#) density  $\rho$ , porosity  $\varphi$ , and saturation  $s$ . The Darcy velocity,  $\mathbf{q}$ , is given by

$$\mathbf{q} = -\frac{kk_r}{\mu} \nabla(p - \rho g z), \quad (2)$$

with [waterliquid](#) pressure  $p$ , viscosity  $\mu$ , acceleration of gravity  $g$ , intrinsic permeability  $k$ , relative permeability  $k_r$  and elevation above a given datum  $z$ . Conservative solute transport in the liquid phase is based on the advection-dispersion equation

$$\frac{\partial}{\partial t}(\varphi s C) + \nabla \cdot (\mathbf{q} - \varphi s D \nabla) C = 0, \quad (3)$$

with [solute](#) concentration  $C$  and hydrodynamic dispersion coefficient  $D$ . [PFLOTRAN](#) ~~employs backward Euler time discretization and finite volume spatial discretization.~~ The [discrete](#)

~~system discretized set of nonlinear equations PDEs for flow and transport are solved by using the Newton-Raphson method.~~

### 2.3 Model coupling

~~For the coupled PFLOTRAN\_CLM v1.0 model In this workstudy, CLM4.5's one-dimensional models for flow in unsaturated [Zeng and Decker, 2009] and saturated [Niu et al., 2007] zones are replaced by PFLOTRAN's RICHRADS mode to simulate unsaturated-saturated flow within the describes the subsurface flow and solute transport three-dimensional subsurface domain. while CLM4.5 simulates the land surface processes. Although, PFLOTRAN is also capable of simulating coupled flow and thermal processes in the subsurface including explicit representation of liquid-ice phase [Karra et al., 2014], as well as, The soil carbon and nitrogen nutrient cycling, [Hammond and Lichtner, 2010; Zachara et al., 2016; Tang et al., 2016], can be solved in either PFLOTRAN or CLM4.5 but those processes are not enabled coupled between the two models in this study. A schematic representation of the coupling between PFLOTRAN and CLM4.5 (within the CESM1 framework) is shown in top panel of Figure 1.~~

~~A schematic representation of the coupling between CLM4.5 and PFLOTRAN is shown in Figure 1. A model coupling interface layer based on PETSc data structures was developed to couple PFLOTRAN and CLM4.5, the two models and the interface including some key design features of the CESM coupler [Craig et al., 2012]. The model coupling interface to support allows each model grid to have a different spatial resolution and domain decomposition across multiple processors. (i) different model domain decompositions and (ii) different grid resolutions. Both models support distributed memory parallelism via MPI, but perform domain decomposition across multiple processors differently. While CLM4.5 uses a round-robin decomposition approach, PFLOTRAN employs domain decomposition via PETSc (Figure 1a). Interpolation of gridded data from one model's grid onto the grids of the other's grid is done through sparse matrix vector multiplication. The model interface is developed to allow each model to support its native domain decomposition when run as a coupled model. The interface also allows the two models to run on different resolution grids and uses mapping files to regrid data for transfer between the two models. As a preprocessing step, sparse weight matrices for interpolating data between the two models are saved as mapping files. Analogous to the CESM~~

coupler, the mapping files are ~~saved generated as a pre-processing step~~ in a format similar to the mapping files produced by the ESMF\_RegridWeightGen (<https://www.earthsystemcog.org/projects/regridweightgen>). [ESMF regridding tools provides multiple interpolation methods \(conservative, bilinear, and nearest neighbor\) to generate the sparse weight matrix.](#) In this work, we have used a conservative remapping method to interpolate data between CLM and PFLOTRAN. During model initialization, ~~the model coupling interface first uses PETSc data structures to efficiently collectively reads all required sparse matrices.~~ Next, the model coupling interface reassembles local sparse matrices after accounting for domain decomposition of each model (figures 1b and 1c). ~~handle cross-processor communication and sparse matrix-vector products for mapping data from one grid to another.~~

For a given time step, CLM4.5 first computes infiltration, evaporation, and transpiration within the domain ~~and then sends the data to the model coupling interface.~~ ~~The CLM4.5 simulated water sources and sinks are then~~ The model coupling interface for each processor receives relevant CLM data vector from all other processors; ~~interpolates data from CLM's grid onto PFLOTRAN's grid via a local sparse matrix vector multiplication; and saves the resulting vector in PFLOTRAN's data structures as prescribed flow conditions (Figure 1b).~~ PFLOTRAN evolves the subsurface states over the given time step length. ~~used as prescribed conditions in the flow and transport simulation by PFLOTRAN.~~ The ~~updated~~ soil moisture ~~and soil hydraulic properties~~ simulated by PFLOTRAN are then provided ~~back~~ to ~~the model coupling interface,~~ which interpolates data from PFLOTRAN's grid onto CLM's grid (Figure 1c). ~~The interpolated data is saved in CLM4.5's data structure and used~~ for simulating land water- and energy- budget terms in the next step. [Figure 2](#) shows a schematic representation of how stream-aquifer-land interactions are simulated in [PFLOTRAN-CLM-PFLOTRAN-SIZCP](#) v1.0 when applied to the field scale, such as the 300 Area domain to be introduced in section 3.1.

### 3 Site description and model configuration

#### 3.1 The Hanford site and the 300 Area

The Hanford Reach is a stretch of the lower Columbia River extending approximately 55 km from the Priest Rapids hydroelectric dam to the outskirts of Richland, Washington, USA (Figure

[2a3a](#)) [Tiffan *et al.*, 2002]. The Columbia River above Priest Rapids Dam drains primarily mountainous regions in Canada, Idaho, Montana, and Washington, over which spatio-temporal distributions of precipitation and snowmelt modulate the timing and magnitude of river flows [Elsner *et al.*, 2010; Hamlet and Lettenmaier, 1999]. The Columbia River is highly regulated by dams for power generation and river stage and discharge along the Hanford Reach displays significant variation on multiple time scales. Strong seasonal variations occur with the greatest discharge (up to  $12,000 \text{ m}^3 \text{ s}^{-1}$ ) occurring from May through July due to snow melt, with less discharge ( $>1,700 \text{ m}^3 \text{ s}^{-1}$ ) and lower flows occurring in the fall and winter [Hamlet and Lettenmaier, 1999; Waichler *et al.*, 2005]. Significant variation in discharge also occurs on a daily or hourly basis due to power generation, with fluctuations in river stage of up to 2 m within a 6-24 hr period being common [Tiffan *et al.*, 2002].

The Hanford site features an unconfined aquifer developed in Miocene-Pliocene fluvial and lacustrine sediments of the Ringold Formation, overlain by Pleistocene flood gravels of the Hanford formation [Thorne *et al.*, 2006] that is in hydrologic continuity with the Columbia River. The Hanford formation gravel and sand, deposited by glacial outburst floods at the end of the Pleistocene [Bjornstad, 2007], has a high average hydraulic conductivity at  $\sim 3,100 \text{ m day}^{-1}$  [Williams *et al.*, 2008]. The fluvial deposits of the Ringold Formation have much lower hydraulic conductivity than the Hanford but are still relatively conductive at  $36 \text{ m day}^{-1}$  [Williams *et al.*, 2008]. Fine-grained lacustrine Ringold silt has a much lower estimated hydraulic conductivity of  $1 \text{ m day}^{-1}$ . The hydraulic conductivity of recent alluvium lining the river channel is low relative to the Hanford formation, which tends to dampen the response of water table elevation in wells near the river when changes occur in river stage [Hammond *et al.*, 2011; Williams *et al.*, 2008]. Overall, the Columbia River through the Hanford Reach is a prime example of a hyporheic corridor with an extensive floodplain aquifer. It is consequently an ideal alluvial system for evaluating the capability of the coupled model in simulating stream-aquifer-land interactions.

The region is situated in a cold desert climate with temperatures, precipitation, and winds that are greatly affected by the presence of mountain barriers. The Cascade Range to the west creates a strong rain shadow effect by forming a barrier to moist air moving from the Pacific Ocean, while the Rocky Mountains and ranges to the north protect it from the more severe cold polar air masses and winter storms moving south across Canada. Meteorological data are collected by the

Hanford Meteorological Monitoring Network (<http://www.hanford.gov/page.cfm/hms>), which collects meteorological data representative of the general climatic conditions for the Hanford site.

A segment of the hyporheic corridor in the Hanford 300 Area (300A) was chosen to evaluate the model's capability in simulating river-aquifer-land interactions. Located at the downstream end of the Hanford Reach, the impact of dam operations on river stage is relatively damped, exhibiting a typical variation of ~0.5 m within a day and 2-3 m in a year. The study domain covers an area of 400 m × 400 m along the Columbia River shoreline (-Figure 23(b)). Aquifer sediments in the 300 Area are coarse grained and highly permeable [*Chen et al., 2013; Hammond and Lichtner, 2010*]. Coupled with dynamic river stage variations, the resulting system is characterized by stage-driven intrusion and retreat of river water into the adjacent unconfined aquifer system. During high-stage spring runoff events, river water has been detected in monitoring wells nearly 400 m from the shoreline [*Williams et al., 2008*]. During baseline, low-stage conditions (October-February), the Columbia River is a gaining stream, and the aquifer pore space is occupied by groundwater.

The study domain is instrumented with groundwater monitoring wells (Figure 2b3b) and a river gaging station that records water table elevations. A vegetation survey in 2015 was conducted to provide aerial coverages of grassland, shrubland, riparian trees in the domain (Figure 2b3b). A high-resolution topography and bathymetry dataset at 1-m resolution was assembled from multiple surveys by *Coleman et al.* [2010]. The data layers originated from Deep Water Bathymetric Boat surveys, terrestrial Light Detection and Ranging (LiDAR) surveys, and special hydrographic LiDAR surveys penetrating through water to collect both topographic and bathymetric elevation data.

### 3.2 Model configuration, numerical experiments, and analyses

To assess the effect of spatial resolution on simulated variables such as latent heat, sensible heat, water table depth, and river water in the domain, we configured ~~PFL~~PFL~~OTRAN\_CLM\_PFL~~OTRAN\_SIZCP v1.0 simulations at three horizontal spatial resolutions: 2-m, 10-m, and 20-m over the 400 m×400 m domain, respectively. For comparison purposes, we also configured a 2-m-resolution ~~CLM\_PFL~~OTRAN\_SIZCP~~PFL~~OTRAN\_CLM v1.0 vertical only simulation (i.e., ~~PF~~CLM<sub>v2m</sub>~~S~~v2m) in which lateral transfers of flow and solutes in the

subsurface are disabled. Due to lack of observations of water and energy fluxes from the land surface, in this study we treat the 2-m-resolution [CLM\\_PFLOTRAN\\_SIZCPPFLOTRAN\\_CLM v1.0](#) as the baseline and compare simulation results at other resolutions to it. New hydrologic regimes are projected to emerge over the Pacific Northwest in as early as the 2030s due to increases in winter precipitation and earlier snow melt in response to future warming [*Leng et al.*, 2016a]. Therefore, we expect that spring and early summer river discharge along the reach might increase in the future. To evaluate how land surface-subsurface coupling might be modulated hydro-climatic conditions, we designed additional numerical experiments by driving the model with elevated river stages by adding five meters to the observed river stage time series. The simulations and their configurations are summarized in Table 1.

The PFLOTRAN subsurface domain, also terrain-following and extending from soil surface (including riverbed) to 32 m below the surface, was discretized using a structured approach with rectangular grids. For the 2-m, 10-m, and 20-m resolution simulations, each mesh element was 2 m  $\times$  2 m, 10 m  $\times$  10 m, and 20 m  $\times$  20 m, in the horizontal direction, and 0.5 m in the vertical direction, giving  $2.56 \times 10^6$ ,  $99.2 \times 10^3$ , and  $2.48 \times 10^3$  control volumes in total. The domain contained two materials with contrasting hydraulic conductivities: Hanford and Ringold (Figure [34](#)). Note that only the soil moisture and soil hydraulic properties within the top 3.8 m are transferred from PFLOTRAN to CLM4.5 to allow simulations of infiltration, evaporation, and transpiration in the next time step, as the CLM4.5 subsurface domain is limited to 3.8 meters and cannot currently be easily modified. The hydrogeological properties of the Hanford and Ringold materials (Table 2) were taken from *Williams et al.* [2008]. The unsaturated hydraulic conductivity in PFLTORAN simulations was computed using the Van Genuchten water retention function [*van Genuchten*, 1980] and the Burdine permeability relationship [*Burdine*, 1953].

We applied time varying pressure boundary conditions to PFLOTRAN's subsurface domain at the northern, western, and southern boundaries. The transient boundary conditions were derived using kriging-based interpolations of hourly water table elevation measurements in wells inside and beyond the model domain, following the approach used by *Chen et al.* [2013]. Transient head boundary conditions were applied at the eastern boundary with water table elevations from the river gaging station and the gradient along the river estimated using water elevations simulated by a 1-D hydraulic model along the reach, the Modular Aquatic Simulation System in 1-Dimension (MASS1) [*Waichler et al.*, 2005], with a Nash–Sutcliffe coefficient

[*Nash and Sutcliffe, 1970*] of 0.99 in the simulation period (figure not shown). The river stage simulated by MASS1 was also used to fill river stage measurement gaps caused by instrument failures. A conductance value of  $10^{-12}$  m was applied to the eastern shoreline boundary to mimic the damping effect of low-permeability material on the river bed [*Hammond and Lichtner, 2010*]. A no-flow boundary condition was specified at the bottom of the domain to represent the basalt underlying the Ringold formation.

Vegetation types (Figure 23(b)) were converted to corresponding CLM4.5 plant functional types (PFTs) and bare soil (Figure 45). At each resolution, fractional area coverages of PFTs and bare soil are determined based on the base map and written into the surface dataset as CLM4.5 inputs (figures 45, S1, and S2). The CLM4.5 domain is terrain-following by treating the land surface as the top of the subsurface domain, which is hydrologically active to a depth of 3.8 m. The topography of the domain is retrieved from the 1-m topography and bathymetry dataset [*Coleman et al., 2010*] based on the North American Vertical Datum of 1988 (NAD88) and resampled to each resolution (Figure S3).

The simulations were driven by hourly meteorological forcing from the Hanford meteorological stations and hourly river stage from the gaging station over the period of 2009-2015. Precipitation, wind speed, air temperature, and relative humidity were taken from the 300 Area meteorological station (longitude 119.726°, latitude 46.578°), located ~1.5 km from the modeling domain. Other meteorological variables, such as downward shortwave and longwave radiation, were obtained from the Hanford Meteorological station (longitude 119.599°, latitude 46.563°) located in the center of the Hanford site. The first two years of simulations (i.e., 2009 and 2010) were discarded as the spin-up period, so that 2011-2015 is treated as the simulation period in the analyses.

Among the hydro-climatic forcing variables (e.g., river stage, surface air temperature, incoming shortwave radiation, and total precipitation), river stage displayed the greatest inter-annual variability (Figure 56). During the study period, high river stages occurred in early summer of 2011 and 2012 due to the melt of above-average winter snow packs in the upstream drainage basin, typical flow conditions occurred in 2013 and 2014, while 2015 was a year with low upstream snow accumulation. Meanwhile, the meteorological variables, especially temperature and shortwave radiation, do not show much inter-annual variability or trend, while

precipitation in late spring (i.e., May) of 2012 is higher than that in the other years, coincident with the high river stage in 2012. In the “elevated” experiments (i.e., [PFCLM<sub>E2m</sub>S<sub>E2m</sub>](#), [PFCLM<sub>E10m</sub>S<sub>E10m</sub>](#), and [PFCLM<sub>E20m</sub>S<sub>E20m</sub>](#)), the observed river stage (meters based on NAD88) was increased by five meters at each hourly time step to mimic a perturbed hydro-climatic condition in response to future warming.

To evaluate effects of river water and groundwater exchanges on land surface energy partitioning, we separated the study domain for the 2-m simulations with lateral water exchange (i.e., [PFCLM<sub>2m</sub>S<sub>2m</sub>](#) and [PFCLM<sub>E2m</sub>S<sub>E2m</sub>](#)) into two sub-domains based on 2-m topography (shown in Figure S3a): (a) the inland domain where the surface elevation is higher than 110 m; and (b) the riparian zone where the surface elevation is less than or equal to 110 m. In addition to the latent heat flux, the [Bowen ratio/evaporative fraction](#), defined as the ratio [between-of](#) the [sensible-latent](#) heat flux [and-to](#) the sum of latent and sensible heat fluxes [latent heat flux](#), was calculated over the sub-domains for both observed and elevated conditions [in-the-warm-months](#) (i.e., [April-to-September](#)) at a daily time step. [The-cold-months-were-not-included-in-this-analysis](#) to avoid numerical issues as a result of low energy inputs in combinations with water limitation [in-the-winter, when LH could potentially become zero for all days with significant energy inputs](#) (i.e., when net radiation is greater than 50 W m<sup>2</sup>). The [Bowen ratio/evaporative](#) is an indicator of the type of surface as summarized in literature [Lewis, 1995]: it is typically less than one over surfaces with abundant water supplies, ranges between [0.1-0.30.75-0.9](#), [0.40.5-0.78](#), [2.00.15-6.00.3](#) for tropical rainforests, temperate forests and grasslands, semi-arid landscapes, respectively, and [becomes >10.0 approaches 0](#) over deserts.

To better quantify the spatio-temporal dynamics of stream-aquifer interactions, a conservative tracer with a mole fraction of one was applied at the river boundary to track the flux of river water and its total mass in the subsurface domain. While a constant concentration was maintained at the river (i.e., eastern) boundary, the tracer was allowed to be transported out of the northern, western, and southern boundaries. Water infiltrating at the upper boundary based on CLM4.5 simulations was set to be tracer free, while a zero-flux tracer boundary condition was applied at the lower boundary. The initial flow condition was a hydrostatic pressure distribution based on the water table, as interpolated from the same set of wells that were used to create the transient lateral flow boundary conditions at the northern, western, and southern boundaries. The initial conservative tracer concentration was set to be zero for all mesh elements in the domain.

The simulations were started on 1 January 2009 and the first two years were discarded as the spin-up period in the analysis. The mass of tracers in the domain and the fluxes of tracers across the boundary allow us to quantitatively understand how river water is retained and transported in the subsurface domain.

A standalone CLM4.5 simulation was also configured and performed (i.e., CLM<sub>2m</sub> in Table 1). CLM<sub>2m</sub> shared the same subsurface properties and initial conditions as the CLM4.5 setup in S<sub>2m</sub> and S<sub>v2m</sub> where CP v1.0 were used. However, we note that CLM<sub>2m</sub> are not directly comparable to other simulations listed in Table 1 for following reasons: (1) The CLM4.5 simulates subsurface hydrologic processes only up to 3.8 m below the surface, while in the CP v1.0 -subsurface domain extends up to ~30 m below the surface; (2) as discussed in section 2.1, ~~in~~, CLM4.5 uses TOPMODEL-based parameterizations to simulate surface and subsurface runoffs, as well as mean groundwater table depth using formulations derived from catchment hydrology that are only applicable at coarser resolutions; (3) The key hydrologic processes (i.e., the exchange of river water and groundwater at the east boundary and lateral transfer of water at all other boundaries) that affect the hydrologic budget of the system are missing from CLM4.5. Therefore, the simulated latent heat fluxes from CLM<sub>2m</sub> are only provided as a reference for interested readers in Figure S4 and were not analyzed in section 4.

## 4 Results

### 4.1 Model ~~validation~~ evaluation

For the 3-D numerical experiments driven by the observed river stage time series (i.e., ~~PFCLM<sub>2m</sub>S<sub>2m</sub>, PFCLM<sub>10m</sub>S<sub>10m</sub>, PFCLM<sub>20m</sub>S<sub>20m</sub>~~), CLM\_PFLOTRAN\_SIZCPPFLTORAN\_CLM v1.0 simulated soil water pressure was converted to water table depth and compared against observed values at selected wells that were distributed throughout the domain and of variable distances from the river (~~Figure f~~Figures 6-7, S5 and Table 3). The model performed very well in simulating the temporal dynamics of the water table at all resolutions. The root-mean-square errors were 0.028 m, 0.028 m, and 0.023 m at 2-m, 10-m, and 20-m resolutions, respectively. The corresponding Nash–Sutcliffe coefficients were 0.998, 0.998, and 0.999. It was surprising that the performance metrics at 20-m resolution ~~outperform~~ matches the observations better than

those at finer resolutions, but the differences were marginal given the close match between the model [simulation results](#) and observations. River stage was clearly the dominant driving factor for water table fluctuations at the inland wells. [In addition, errors in water and tracer budget conservations, and surface energy conservation for each time step in  \$S\_{2m}\$  are shown in figures S6a, b, and c respectively. The errors are sufficiently small when compared to the magnitudes of the related fluxes to ensure faithful simulations in CP v1.0.](#) These results indicated that the coupled model was capable of simulating dynamic stream-aquifer interactions in the near shore groundwater aquifer that experiences pressure changes induced by river stage variations at sub-daily time scales.

## 4.2 Effect of stream-aquifer interactions on land surface energy partitioning

Next we evaluated the role of water table fluctuations on land surface variables, including latent heat (LH) and sensible heat (SH) fluxes. The site is characterized by an approximate 10 m vadose zone and surface fluxes and groundwater dynamics are typically decoupled [*Maxwell and Kollet, 2008*], especially over the inland portion of the domain covered by shallow-rooted PFTs and with higher surface elevations. However, river discharge and water table elevation displayed large seasonal and inter-annual variability in the study period. Therefore, we selected the month of June in each year to assess potential land surface-groundwater coupling because it is the month of peak river stage, while energy input is high and relatively constant across the years (Figure [7a8a](#)).

In June 2011 and 2012, high river stages push the groundwater table to ~108 m (or ~6 m below the land surface). Groundwater at that elevation can affect land surface water and energy exchanges with the atmosphere. The shrubs, including the patch of Basin big sagebrush and the mixture of rabbitbrush and bunchgrass on the slope close to the river, are able to tap into the elevated water table with their deeper roots. In the inland portion of the domain, capillary supply was most evident in high-water years (i.e., 2011 and 2012), remains influential in normal years (i.e., 2013 and 2014), and is essentially disabled in low-water years (i.e., 2015). The lateral discharge of shallow groundwater to the river led to a band of negative difference in LH between [PFCLM<sub>2m</sub>-S<sub>2m</sub>](#) and [PFCLM<sub>v2m</sub>-S<sub>v2m</sub>](#) at the river boundary when the stage was low due to a

decrease in rooting zone soil moisture for evapotranspiration by the riparian trees (Figure 7b8b). This pattern was most evident in June 2015. Such a mechanism decreases in high-water and normal years because of more frequent inundation of the river bank and groundwater gradient reversal.

Driven by elevated river stages, land surface energy partitioning in  $PFCLM_{E2m-S_{E2m}}$  (figures [Figure 8-9](#) and [910](#)) was significantly shifted from that in  $PFCLM_{2m-S_{2m}}$  (Figure 7a8a) through two mechanisms: (1) expanding the periodically inundated fraction of the riparian zone (i.e., surface elevation  $\leq 110$  m); and (2) enhancing moisture availability in the vadose zone in the inland domain (i.e., surface elevation  $> 110$  m) through capillary rise. Both mechanisms led to general increases in simulated vadose-zone moisture availability and therefore higher latent heat fluxes compared to the simulations driven by the observed condition. For the inland domain, ~~Bowen ratios in the warm season~~ evaporative fraction clearly displayed ~~a declining~~ an increasing trend as the groundwater table level ~~increased (i.e., shallower)~~ becomes shallower, consistent between the simulations (Figure [9a10c](#)). ~~75% of the~~ The daily ~~Bowen ratio~~ evaporative fractions for the inland domain stayed ~~mostly > 5.0~~ well below 0.2 when the water table levels are less than ~~108–112~~ m, suggesting decoupled surface-subsurface conditions in a typical semi-arid environment. When water table levels increased to be above ~~108–112~~ m, ~~the coupling between the land surface energy budget and groundwater dynamics became stronger~~ the evaporative fraction increases to ~0.2. ~~As the elevation of the land surface is around 114–115 m~~, indicating that ~~the water table fluctuated within the 6 m to 7 m range from the land surface~~, the surface and subsurface processes ~~were become more strongly coupled~~, consistent with literature findings [Leung et al., 2011; Maxwell and Kollet, 2008]. Consequently, ~~50–75% of the daily Bowen ratio values stayed well below 5.0~~ because of improved water availability for evapotranspiration, especially in the elevated simulation (i.e.,  $PFCLM_{E2m-S_{E2m}}$ ). ~~Bowen-Evaporative fraction ratios~~ in the riparian zone remained ~~within the range of [-1.0, 1.0]~~ close to 1.0, suggesting strong influences of the river and the role of deeper rooted plant types (e.g., riparian trees and shrubs) in modulating the energy partitioning (Figure [910d](#)) of riparian zones in the semi-arid to arid environments.

To confirm the above findings, the liquid saturation [*unitless*] and mass of river water [*mol*] in the domain from  $PFCLM_{2m-S_{2m}}$  and  $PFCLM_{E2m-S_{E2m}}$  on 30 June each year are plotted along a transect perpendicular to the river ( $y = 200$  m) in figures [10-11](#) and [S4S7](#), and across a x-y plane

at an elevation of 107 m in figures [S5-S8](#) and [S6S9](#), respectively. Driven by the pressure introduced by elevated river stages, river water not only intruded further toward or even across the western boundary in high water years, but also led to shallower water table and increased liquid saturation in the vadose zone due to capillary rise across the domain. In fact, liquid saturation in the shallow vadose zone could increase from 0.1-0.2 in [PFCLM<sub>2m</sub>-S<sub>2m</sub>](#) to 0.3-0.4 in [PFCLM<sub>E2m</sub>-S<sub>E2m</sub>](#) on these days because of river water intrusion. ~~And t~~The river-water tracer could show up in the near-surface vadose zone at a distance of ~400 m from the river (Figure [S4S7](#)). Interestingly, by comparing the spatial distributions of river-water tracer in the low-water year (i.e., 2015) between the “observed” and “elevated” scenarios, the presence of river water in the domain was much less in the elevated scenario in terms of its spatial coverage (figures [10-11](#) and [S4S7](#)). This pattern suggests that after a number of years of enhanced river water intrusion into the domain, the hydraulic gradient between groundwater and river-water could be reversed, so that groundwater discharging might be expected more frequently in low-water years in a prolonged elevated scenario.

The responses of LH and ~~Bowen ratio~~evaporative fraction (figures [8-9](#) and [910](#)) indicated that a tight coupling among stream, aquifer, and land surface processes occurred in the elevated scenario, which could become realistic in one to two decades for the study site, or for other sites along the Hanford reach characterized by lower elevations under the current condition.

### 4.3 Effect of spatial resolution

To apply the model to large-scale simulations or over a long time period, it is important to assess how the model performs at coarser resolution, as the 2-m simulations are computationally expensive. Here, we use the 2-m simulations (i.e., [PFCLM<sub>2m</sub>-S<sub>2m</sub>](#) and [PFCLM<sub>E2m</sub>-S<sub>E2m</sub>](#)) simulations as benchmarks for this assessment. That is, [PFCLM<sub>2m</sub>-S<sub>2m</sub>](#) and [PFCLM<sub>E2m</sub>-S<sub>E2m</sub>](#) simulated variables are treated as the “truth” for “observed” and “elevated” river stage scenarios, and outputs from other simulations are compared to them to verify their performance. In the previous section, we showed that simulated water table levels from the model were virtually identical to observations. In this section, we further quantify biases of other variables of interest from the high-fidelity 2-m simulations.

The domain-averaged daily surface energy fluxes from [PFCLM<sub>2m</sub>-S<sub>2m</sub>](#) show clear seasonal patterns, which are consistent in terms of their magnitudes and timing, reflecting mean climate conditions at the site (Figure [S6S10](#)). Driven by elevated river stages, latent heat from [PFCLM<sub>E2m</sub>-S<sub>E2m</sub>](#) is consistently higher than that from [PFCLM<sub>2m</sub>-S<sub>2m</sub>](#). The mean latent heat and sensible heat fluxes simulated by [PFCLM<sub>2m</sub>-S<sub>2m</sub>](#) were  $14.1 \text{ W m}^{-2}$  and  $38.7 \text{ W m}^{-2}$  over this period, compared to by  $18.50 \text{ W m}^{-2}$  and  $35.75 \text{ W m}^{-2}$  in [PFCLM<sub>E2m</sub>-S<sub>E2m</sub>](#). Figure [4-12](#) shows deviations of simulated LH and SH in the 20-m and 10-m simulations from the corresponding 2-m simulations. The deviations of both LH and SH were small across all the simulations driven by the observed river stage when surface and subsurface were decoupled. In the elevated simulations (i.e., [PFCLM<sub>E10m</sub>-S<sub>E10m</sub>](#) and [PFCLM<sub>E20m</sub>-S<sub>E20m</sub>](#)) when surface and subsurface processes are more tightly coupled, errors in surface fluxes became significant in the coarse resolution simulations when compared to [PFCLM<sub>E2m</sub>-S<sub>E2m</sub>](#). For example, the relative errors in LH were 2.41% and 1.35% for [PFCLM<sub>20m</sub>-S<sub>20m</sub>](#) and [PFCLM<sub>10m</sub>-S<sub>10m</sub>](#), respectively, as compared to [PFCLM<sub>2m</sub>-S<sub>2m</sub>](#), but grew as large as 33.84% and 33.19% for [PFCLM<sub>E20m</sub>-S<sub>E20m</sub>](#) and [PFCLM<sub>E10m</sub>-S<sub>E10m</sub>](#), respectively, when compared to [PFCLM<sub>E2m</sub>-S<sub>E2m</sub>](#). The 10-m simulations outperformed the 20-m simulations under both scenarios but the magnitudes of errors were comparable. On the other hand, notably the vertical only simulation ([PFCLM<sub>v2m</sub>-S<sub>v2m</sub>](#)) has a small error of 5.67% in LH compared to [PFCLM<sub>2m</sub>-S<sub>2m</sub>](#), indicating that lateral flow is less important when water table is deep.

To better understand how water in the river and the aquifer was connected, we also quantified the biases of subsurface state variables and fluxes including total water mass and tracer amount, as well as exchange rates of water and tracer at four boundaries of the subsurface domain using a similar approach (Figure [S7-S11](#) and Figure [4-13](#)). Compared to the magnitude of total water mass in the domain (averaged  $919.45 \times 10^6 \text{ Kg}$  and  $1020.19 \times 10^6 \text{ Kg}$  in [PFCLM<sub>2m</sub>-S<sub>2m</sub>](#) and [PFCLM<sub>E2m</sub>-S<sub>E2m</sub>](#)), errors introduced by coarsening the resolution were very small under the observed river stage condition (0.04% for [PFCLM<sub>20m</sub>-S<sub>20m</sub>](#) and 0.03% for [PFCLM<sub>10m</sub>-S<sub>10m</sub>](#)) and grew to 9.85% for [PFCLM<sub>E20m</sub>-S<sub>E20m</sub>](#) and 9.87% for [PFCLM<sub>E10m</sub>-S<sub>E10m</sub>](#) in terms of total water mass in the domain (Table 5). However, for total tracer in the domain (averaged  $142.07 \times 10^6 \text{ mol}$  and  $172.46 \times 10^6 \text{ mol}$  in [PFCLM<sub>2m</sub>-S<sub>2m</sub>](#) and [PFCLM<sub>E2m</sub>-S<sub>E2m</sub>](#)) as a result of transport of river water in lateral and normal directions to the river, resolution clearly makes a difference under both observed condition and elevated scenarios (relative errors of 5.44% for

[PFCLM<sub>10m</sub>S<sub>10m</sub>](#), 10.40% for [PFCLM<sub>20m</sub>S<sub>20m</sub>](#), and 22.0% for both [PFCLM<sub>E10m</sub>-S<sub>E10m</sub>](#) and [PFCLM<sub>E20m</sub>S<sub>E20m</sub>](#)). The magnitude of computed mass exchange rates at the four boundaries (Figure [42S11](#)) indicates that a coarse resolution promotes larger river water fluxes and groundwater exchanges, especially during the period of spring river stage increase under the elevated scenario. This forcing contributes to a significant bias in total tracer amount by the end of the simulation. The exchange rates at the other three boundaries follow the same pattern but with smaller magnitudes, especially for the west boundary that requires a significant gradient high enough to push river water further inland.

The results of simulations at three different resolutions indicated that: (1) the partitioning of the land surface energy budget is mainly controlled by near-surface moisture. Spatial resolution did not seem to be a significant factor in the computation of surface energy fluxes when the water table was deep at the semi-arid site; (2) if the surface and subsurface are tightly coupled as in the elevated river stage simulations, resolution becomes an important factor to consider for credible simulations of the surface fluxes, as the land surface, subsurface, and riverine processes are expected to be more connected and coupled; (3) regardless of whether a tight coupling between the surface and subsurface occurs, if mass exchange rates and associated biogeochemical reactions in the aquifer are of interest, a higher resolution is desired close to the river shoreline to minimize terrain errors.

## 5 [Conclusion Discussion](#) and future work

A [fully](#)-coupled three-dimensional surface and subsurface land model was developed and applied to a site along the Columbia River to simulate interactions among river water, groundwater, and land surface processes. The model features the coupling of the open-source and state-of-the-art models portable on HPCs, the multi-physics reactive transport model PFLOTRAN and the CLM4.5. Both models are under active development and testing by their respective communities, therefore the coupled model could be updated to newer versions of PFLOTRAN and/or CLM to facilitate transfer of knowledge in a seamless fashion. The [integrated-coupled](#) model represents a new addition to the integrated surface and subsurface suite of models.

By applying the coupled model to a field site along the Columbia River shoreline driven by highly dynamic river boundary conditions resulting from upstream dam operations, we

demonstrated that the model can be used to advance mechanistic understanding of stream-aquifer-land interactions surrounding near-shore alluvial aquifers that experience pressure changes induced by river stage variations along managed river reaches, which are of global significance as a result of over 30,000 dams constructed worldwide during the past half century. The land surface, subsurface, and riverine processes along such managed river corridors are expected to be more strongly coupled under projected hydro-climatic regimes as a result of increases in winter precipitation and early snowmelt. The dataset presented in this study can serve as a good benchmarking case for testing other [integrated-coupled](#) models for their applications to such systems. More data needs to be collected to facilitate the application and validation of the model to a larger domain for understanding the contribution of near-shore hydrologic exchange to water retention, biogeochemical cycling, and ecosystem functions along the river corridors.

By benchmarking the coarser resolution simulations at 20 m and 10 m against the 2-m simulations, we find that resolution is not a significant factor for surface flux simulations when the water table is deep. However, resolution becomes important when the surface and subsurface processes are tightly coupled, and for accurately estimating the rate of mass exchange at the riverine boundaries, which can affect the calculation of biogeochemical processes involved in carbon and nitrogen cycles.

Our numerical experiments suggested that riverine, land surface, and subsurface processes could become more tightly coupled through two mechanisms in the near-shore environments: (1) expanding the periodically inundated fraction of the riparian zone and (2) enhancing moisture availability in the vadose zone in the inland domain through capillary rise. Both mechanisms can lead to increases in vadose-zone moisture availability and higher evapotranspiration rates. The latter is critical for understanding ecosystem functioning, biogeochemical cycling, and land-atmosphere interactions along river corridors in arid and semi-arid regions that are expected to experience new hydro-climatic regimes in a changing climate. However, these systems have been poorly accounted for in current-generation Earth system models and therefore require more attention in future studies.

[We acknowledge that there are a number of limitations of this study that need to be addressed in future studies:](#)

(1) Motivated by understanding the stream-aquifer-land interactions with a focus on groundwater and river water interactions along a river corridor situated in a semi-arid climate, the river boundary conditions were prescribed using observations with gaps filled by a 1-D hydrodynamics model. Future versions of the CP model need to incorporate two-way interactions between stream and aquifer by developing a surface flow component and testing the new implementation against standard benchmark cases [Kollet et al., 2017; Maxwell et al., 2014].

(2) We note that CLM estimates the surface heat and moisture fluxes using the Monin-Obukhov Similarity Theory (section 2.1), which is only valid when the surface layer depth  $z \gg z_0$ , where  $z_0$  is the aerodynamic roughness length. As reviewed by Basu and Lacser [2017], it is highly recommended that  $z > 50z_0$ , which should be proportional to the horizontal grid spacing to guarantee the validity of the Monin-Obukhov Similarity Theory [Arnqvist and Bergström, 2015]. In our simulations, the majority of the Hanford 300A domain is covered by bare soil ( $z_0 = 0.01$  m), grass ( $z_0 = 0.013$  m), shrubs ( $z_0 = 0.026$ - $0.043$  m), and riparian trees (varies across the seasons,  $z_0 = 0.008$  m when LAI = 2 in the summer and  $z_0 = 1.4$  when LAI = 0 in the winter). Therefore, a 2-m resolution is sufficiently coarse under most conditions except for the grid cells covered by riparian trees in the winter. Nevertheless, the wintertime latent heat and sensible heat fluxes are nearly zero due to extremely low energy inputs. Therefore, the 2-m simulations supported by the dense groundwater monitoring network at the site provide a valid benchmark for the coarser resolution simulations. For future applications of the coupled model, caution should be taken to evaluate the site condition for the validity of model parameterizations.

(3) We used the simulated surface energy fluxes from  $S_{2m}$  to verify coarser-resolution simulations. The simulated surface energy flux needs to be validated against eddy covariance tower observations, which are not available yet at the site. Nevertheless, we have made initial efforts to install eddy covariance systems at the site (see description in section 3.1 of Gao et al. [2017]) but the processing the flux data is still preliminary. We will report flux observations and validations of the surface energy budget simulations in future studies.

(4) Even when observed fluxes are available for validation, the model structural problems associated with ET parameterizations in CLM4.5 need to be addressed for reasonable simulations of the ET components, especially for the study site. That is, it has been well-

documented that ET simulated by CLM4.5 and CLM4 could be enhanced when vegetation is removed. This ET enhancement over bare soil has been documented as a counter-intuitive bias for most unsaturated soils in CLM4 and CLM4.5 simulations [Lawrence et al., 2012; Tang and Riley, 2013a]. Tang and Riley [2013a] explored a few potential causes for this likely bias (e.g., soil resistance, litter layer resistance, and numerical time step). They found the implementation of a physically based soil resistance lowered the bias slightly, but concluded that the bias remained [Tang and Riley, 2013b]. Meanwhile, in studying ET over semiarid regions, Swenson and Lawrence [2014] proposed another soil resistance formulation to fix this excessive soil evaporation problem within CLM4.5. While their modification improved the simulated terrestrial water storage anomaly and ET when compared to GRACE data and FLUXNET-MTE data, respectively, the empirical nature of the soil resistance proposed could have underestimated the soil resistance variability when compared to other estimates [Tang and Riley, 2013b].

## Code availability

~~PFLOTRAN is open source software. It is distributed under the terms of the GNU Lesser General Public License as published by the Free Software Foundation either version 2.1 of the License, or any later version. It is available at <https://bitbucket.org/pflotran>. CLM4.5 is also open-source software released as part of the Community Earth System Model (CESM) version 1.2 (<http://www.cesm.ucar.edu/models/cesm1.2>). The version of CLM4.5 used in CLM\_PFLOTRAN\_SIZCP v1.0 is a branch from the CLM developer's repository. I—and its functionality is scientifically consistent with descriptions in *Oleson et al.* [2013] with source codes refactored for a modular code design. Additional minor source—codes refactored modifications were added by the authors for a modular code design to support coupling with PFLOTRAN. Permission from the CESM Land Model Working Group has been obtained to release this CLM4.5 development branch but the National Center for Atmospheric Research cannot provide technical support for this version of the code CLM\_PFLOTRAN\_SIZCP v1.0. PFLOTRAN is an open-source software. It is distributed under the terms of the GNU Lesser General Public License as published by the Free Software Foundation either version 2.1 of the License, or any later version. The CP v1.0 has two separate, open-source repositories for CLM4.5 and PFLOTRAN at:~~

- ~~[https://bitbucket.org/clm\\_pflotran/clm-pflotran-trunk](https://bitbucket.org/clm_pflotran/clm-pflotran-trunk)~~
- ~~[https://bitbucket.org/clm\\_pflotran/pflotran-clm-trunk](https://bitbucket.org/clm_pflotran/pflotran-clm-trunk)~~

~~The README guide for the CP v1.0 and dataset used in this study are available from the open-source repository [https://bitbucket.org/pnnl\\_sbr\\_sfa/notes-for-gmd-2017-35](https://bitbucket.org/pnnl_sbr_sfa/notes-for-gmd-2017-35).~~

~~can be obtained from <https://bitbucket.org/xxxx>.~~

~~PFLOTRAN is open source software. It is distributed under the terms of the GNU Lesser General Public License as published by the Free Software Foundation either version 2.1 of the License, or any later version. It is available at <https://bitbucket.org/pflotran>. CLM4.5 is also open source software released as part of the Community Earth System Model (CESM) version 1.2 (<http://www.cesm.ucar.edu/models/cesm1.2>). PFLOTRAN\_CLM v1.0 is under development and will be made available upon request.~~

## **Acknowledgement**

This research was supported by the U.S. Department of Energy (DOE), Office of Biological and Environmental Research (BER), as part of BER's Subsurface Biogeochemical Research Program (SBR). This contribution originates from the SBR Scientific Focus Area (SFA) at the Pacific Northwest National Laboratory (PNNL).

## References

[Arqvist, J., and Bergström, H. \(2015\), Flux-profile relation with roughness sublayer correction, \*Quarterly Journal of the Royal Meteorological Society\*, 141, 1191-1197, 10.1002/qj.2426, 2015.](#)

Balay, S., J. Brown, K. Buschelman, V. Eijkhout, W. D. Gropp, D. Kaushik, M. G. Knepley, L. C. McInnes, B. F. Smith, and H. Zhang (2015), PETSc Users Manual, Tech. Rep. ANL-95/11—Revision 3.5Rep., Argonne, Ill.

[Basu, S., and Lacser, A. \(2017\). A Cautionary Note on the Use of Monin–Obukhov Similarity Theory in Very High-Resolution Large-Eddy Simulations, \*Boundary-Layer Meteorology\*, 163, 351-355, 10.1007/s10546-016-0225-y.](#)

Beven, K. J., and M. J. Kirkby (1979), A physically based, variable contributing area model of basin hydrology / Un modèle à base physique de zone d'appel variable de l'hydrologie du bassin versant, *Hydrological Sciences Bulletin*, 24(1), 43-69, doi:10.1080/02626667909491834.

Bjornstad, B. N. (2007), *On the Trail of the Ice Age Floods: A Geological Field Guide to the Mid-Columbian Basin*, KeoKee, Sandpoint, ID.

Burdine, N. T. (1953), Relative Permeability Calculations From Pore Size Distribution Data, doi:10.2118/225-G.

Chen, X., G. E. Hammond, C. J. Murray, M. L. Rockhold, V. R. Vermeul, and J. M. Zachara (2013), Application of ensemble-based data assimilation techniques for aquifer characterization using tracer data at Hanford 300 area, *Water Resources Research*, 49(10), 7064-7076, doi:10.1002/2012WR013285.

Chen, X., H. Murakami, M. S. Hahn, G. E. Hammond, M. L. Rockhold, J. M. Zachara, and Y. Rubin (2012), Three-dimensional Bayesian geostatistical aquifer characterization at the Hanford 300 Area using tracer test data, *Water Resources Research*, 48(6), n/a-n/a, doi:10.1029/2011WR010675.

Clark, M. P., et al. (2015), Improving the representation of hydrologic processes in Earth System Models, *Water Resources Research*, 51(8), 5929-5956, doi:10.1002/2015WR017096.

Coleman, A., K. Larson, D. Ward, and J. Lettrick (2010), Development of a High-Resolution Bathymetry Dataset for the Columbia River through the Hanford ReachRep. PNNL-19878, Pacific Northwest National Laboratory, Richland, WA.

Condon, L. E., R. M. Maxwell, and S. Gangopadhyay (2013), The impact of subsurface conceptualization on land energy fluxes, *Advances in Water Resources*, 60(0), 188-203, doi:http://dx.doi.org/10.1016/j.advwatres.2013.08.001.

Craig, A. P., M. Vertenstein, and R. Jacob (2012), A new flexible coupler for earth system modeling developed for CCSM4 and CESM1, *International Journal of High Performance Computing Applications*, 26(1), 31-42, doi:10.1177/1094342011428141.

Elsner, M. M., L. Cuo, N. Voisin, J. S. Deems, A. F. Hamlet, J. A. Vano, K. E. B. Mickelson, S. Y. Lee, and D. P. Lettenmaier (2010), Implications of 21st century climate change for the hydrology of Washington State, *Climatic Change*, 102(1-2), 225-260, doi:DOI 10.1007/s10584-010-9855-0.

Fan, Y., H. Li, and G. Miguez-Macho (2013), Global Patterns of Groundwater Table Depth, *Science*, 339(6122), 940-943.

Fan, Y., and G. Miguez-Macho (2011), A simple hydrologic framework for simulating wetlands in climate and earth system models, *Climate Dynamics*, 37(1), 253-278, doi:10.1007/s00382-010-0829-8.

Fischer, H., F. Kloep, S. Wilzcek, and M. T. Pusch (2005), A river's liver - microbial processes within the hyporheic zone of a large lowland river, *Biogeochemistry*, 76(2), 349-371.

Gaillardet, J., P. Regnier, R. Lauerwald, and P. Ciais (2014), Geochemistry of the Earth's surface GES-10 Paris France, 18-23 August, 2014. Carbon Leakage through the Terrestrial-aquatic Interface: Implications for the Anthropogenic CO<sub>2</sub> Budget, *Procedia Earth and Planetary Science*, 10, 319-324, doi:http://dx.doi.org/10.1016/j.proeps.2014.08.025.

[Gao, Z., Russell, E. S., Missik, J. E. C., Huang, M., Chen, X., Strickland, C. E., Clayton, R., Arntzen, E., Ma, Y., and Liu, H. \(2017\). A novel approach to evaluate soil heat flux calculation: An analytical review of nine methods, \*Journal of Geophysical Research: Atmospheres\*, n/a-n/a, 10.1002/2017JD027160.](#)

[Gebler, S., Hendricks Franssen, H. J., Kollet, S. J., Qu, W., and Vereecken, H.: High resolution modelling of soil moisture patterns with TerrSysMP: A comparison with sensor network data, \*Journal of Hydrology\*, 547, 309-331, https://doi.org/10.1016/j.jhydrol.2017.01.048, 2017.](#)

[Gilbert, J. M., Maxwell, R. M., and Gochis, D. J.: Effects of Water-Table Configuration on the Planetary Boundary Layer over the San Joaquin River Watershed, California, \*Journal of Hydrometeorology\*, 18, 1471-1488, 10.1175/jhm-d-16-0134.1, 2017.](#)

Hamlet, A. F., and D. P. Lettenmaier (1999), Effects of climate change on hydrology and water resources in the Columbia River basin, *Journal of the American Water Resources Association*, 35(6), 1597-1623.

Hammond, G. E., and P. C. Lichtner (2010), Field-scale model for the natural attenuation of uranium at the Hanford 300 Area using high-performance computing, *Water Resources Research*, 46(9), n/a-n/a, doi:10.1029/2009WR008819.

Hammond, G. E., P. C. Lichtner, and R. T. Mills (2014), Evaluating the performance of parallel subsurface simulators: An illustrative example with PFLOTRAN, *Water Resources Research*, 50(1), 208-228, doi:10.1002/2012WR013483.

Hammond, G. E., P. C. Lichtner, and M. L. Rockhold (2011), Stochastic simulation of uranium migration at the Hanford 300 Area, *Journal of Contaminant Hydrology*, 120-21, 115-128, doi:DOI 10.1016/j.jconhyd.2010.04.005.

Harvey, J., and M. Gooseff (2015), River corridor science: Hydrologic exchange and ecological consequences from bedforms to basins, *Water Resources Research*, 51(9), 6893-6922, doi:10.1002/2015WR017617.

Hauer, C., Siviglia, A., and Zolezzi, G.: Hydropeaking in regulated rivers – From process understanding to design of mitigation measures, *Science of The Total Environment*, 579, 22-26, https://doi.org/10.1016/j.scitotenv.2016.11.028, 2017.

Hou, Z., M. Huang, L. R. Leung, G. Lin, and D. M. Ricciuto (2012), Sensitivity of surface flux simulations to hydrologic parameters based on an uncertainty quantification framework applied

to the Community Land Model, *Journal of Geophysical Research: Atmospheres* (1984–2012), 117(D15).

Hurrell, J. W., et al. (2013), The Community Earth System Model: A Framework for Collaborative Research, *Bulletin of the American Meteorological Society*, 94(9), 1339-1360, doi:10.1175/bams-d-12-00121.1.

Ji, X., C. Shen, and W. J. Riley (2015), Temporal evolution of soil moisture statistical fractal and controls by soil texture and regional groundwater flow, *Advances in Water Resources*, 86, Part A, 155-169, doi:http://dx.doi.org/10.1016/j.advwatres.2015.09.027.

[Karra, S., Painter, S. L., and Lichtner, P. C. \(2014\). Three-phase numerical model for subsurface hydrology in permafrost-affected regions \(PFLOTRAN-ICE v1.0\), \*The Cryosphere\*, 8, 1935-1950, 10.5194/tc-8-1935-2014, 2014.](#)

[Keune, J., Gasper, F., Goergen, K., Hense, A., Shrestha, P., Sulis, M., and Kollet, S. \(2016\), Studying the influence of groundwater representations on land surface-atmosphere feedbacks during the European heat wave in 2003, \*Journal of Geophysical Research: Atmospheres\*, 121, 13,301-313,325, 10.1002/2016JD025426, 2016.](#)

Kollet, S. J., and R. M. Maxwell (2008), Capturing the influence of groundwater dynamics on land surface processes using an integrated, distributed watershed model, *Water Resources Research*, 44(2), n/a-n/a, doi:10.1029/2007WR006004.

[Kollet, S., Sulis, M., Maxwell, R. M., Paniconi, C., Putti, M., Bertoldi, G., Coon, E. T., Cordano, E., Endrizzi, S., Kikinzon, E., Mouche, E., Mügler, C., Park, Y.-J., Refsgaard, J. C., Stisen, S., and Sudicky, E. \(2017\).: The integrated hydrologic model intercomparison project, IH-MIP2: A second set of benchmark results to diagnose integrated hydrology and feedbacks, \*Water Resources Research\*, 53, 867-890, 10.1002/2016WR019191.](#)

Kumar, J., N. Collier, G. Bisht, R. T. Mills, P. E. Thornton, C. M. Iversen, and V. Romanovsky (2016), Modeling the spatiotemporal variability in subsurface thermal regimes across a low-relief polygonal tundra landscape, *The Cryosphere*, 10(5), 2241-2274, doi:10.5194/tc-10-2241-2016.

[Lawrence, P. J., Feddesma, J. J., Bonan, G. B., Meehl, G. A., O'Neill, B. C., Oleson, K. W., Levis, S., Lawrence, D. M., Kluzek, E., Lindsay, K., and Thornton, P. E. \(2012\). Simulating the Biogeochemical and Biogeophysical Impacts of Transient Land Cover Change and Wood Harvest in the Community Climate System Model \(CCSM4\) from 1850 to 2100, \*Journal of Climate\*, 25, 3071-3095, 10.1175/jcli-d-11-00256.1.](#)

Lei, H., M. Huang, L. R. Leung, D. Yang, X. Shi, J. Mao, D. J. Hayes, C. R. Schwalm, Y. Wei, and S. Liu (2014), Sensitivity of global terrestrial gross primary production to hydrologic states simulated by the Community Land Model using two runoff parameterizations, *Journal of Advances in Modeling Earth Systems*, 6(3), 658-679.

Leng, G., M. Huang, N. Voisin, X. Zhang, G. R. Asrar, and L. R. Leung (2016a), Emergence of new hydrologic regimes of surface water resources in the conterminous United States under future warming, *Environmental Research Letters*, 11(11), 114003.

Leng, G., X. Zhang, M. Huang, Q. Yang, R. Rafique, G. R. Asrar, and L. R. Leung (2016b), Simulating county-level crop yields in the conterminous United States using the community land model: The effects of optimizing irrigation and fertilization, *Journal of Advances in Modeling Earth Systems*, n/a-n/a, doi:10.1002/2016MS000645.

- Leung, L. R., M. Huang, Y. Qian, and X. Liang (2011), Climate–soil–vegetation control on groundwater table dynamics and its feedbacks in a climate model, *Climate Dynamics*, 36(1), 57-81.
- Lewis, J. M. (1995), The Story behind the Bowen Ratio, *Bulletin of the American Meteorological Society*, 76(12), 2433-2443, doi:10.1175/1520-0477(1995)076<2433:tsbtbr>2.0.co;2.
- Liang, X., D. P. Lettenmaier, E. F. Wood, and S. J. Burges (1994), A simple hydrologically based model of land surface water and energy fluxes for general circulation models, *Journal of Geophysical Research: Atmospheres*, 99(D7), 14415-14428, doi:10.1029/94JD00483.
- Lichtner, P. C., and G. E. Hammond (2012), Using High Performance Computing to Understand Roles of Labile and Nonlabile Uranium(VI) on Hanford 300 Area Plume Longevity, *Vadose Zone Journal*, 11(2), doi:10.2136/vzj2011.0097.
- Lichtner, P. C., G. E. Hammond, C. Lu, S. Karra, G. Bisht, B. Andre, R. T. Mills, and K. Jitu (2015), PFLOTRAN User Manual: a Massively Parallel Reactive Flow and Transport Model for Describing Surface and Subsurface Processes *Rep.*
- Liu, Y., G. Bisht, Z. M. Subin, W. J. Riley, and G. S. H. Pau (2016), A Hybrid Reduced-Order Model of Fine-Resolution Hydrologic Simulations at a Polygonal Tundra Site, *Vadose Zone Journal*, 15(2).
- Maxwell, R. M., and L. E. Condon (2016), Connections between groundwater flow and transpiration partitioning, *Science*, 353(6297), 377-380, doi:10.1126/science.aaf7891.
- Maxwell, R. M., L. E. Condon, and S. J. Kollet (2015), A high-resolution simulation of groundwater and surface water over most of the continental US with the integrated hydrologic model ParFlow v3, *Geosci. Model Dev.*, 8(3), 923-937, doi:10.5194/gmd-8-923-2015.
- Maxwell, R. M., and S. J. Kollet (2008), Interdependence of groundwater dynamics and land-energy feedbacks under climate change, *Nature Geosci.*, 1(10), 665-669.
- Maxwell, R. M., and N. L. Miller (2005), Development of a Coupled Land Surface and Groundwater Model, *Journal of Hydrometeorology*, 6(3), 233-247, doi:10.1175/JHM422.1.
- Maxwell, R. M., et al. (2014), Surface-subsurface model intercomparison: A first set of benchmark results to diagnose integrated hydrology and feedbacks, *Water Resources Research*, 50(2), 1531-1549, doi:10.1002/2013WR013725.
- McNamara, J. P., D. Chandler, M. Seyfried, and S. Achet (2005), Soil moisture states, lateral flow, and streamflow generation in a semi-arid, snowmelt-driven catchment, *Hydrological Processes*, 19(20), 4023-4038, doi:10.1002/hyp.5869.
- Miguez-Macho, G., and Y. Fan (2012), The role of groundwater in the Amazon water cycle: 1. Influence on seasonal streamflow, flooding and wetlands, *Journal of Geophysical Research: Atmospheres*, 117(D15), n/a-n/a, doi:10.1029/2012JD017539.
- Nash, J. E., and J. V. Sutcliffe (1970), River flow forecasting through conceptual models part I — A discussion of principles, *Journal of Hydrology*, 10(3), 282-290, doi:http://dx.doi.org/10.1016/0022-1694(70)90255-6.

- Nir, Y. K., L. Haibin, and F. Ying (2014), Groundwater flow across spatial scales: importance for climate modeling, *Environmental Research Letters*, 9(3), 034003.
- Niu, G.-Y., C. Paniconi, P. A. Troch, R. L. Scott, M. Durcik, X. Zeng, T. Huxman, and D. C. Goodrich (2014), An integrated modelling framework of catchment-scale ecohydrological processes: 1. Model description and tests over an energy-limited watershed, *Ecohydrology*, 7(2), 427-439, doi:10.1002/eco.1362.
- Niu, G.-Y., Z.-L. Yang, R. E. Dickinson, and L. E. Gulden (2005), A simple TOPMODEL-based runoff parameterization (SIMTOP) for use in global climate models, *Journal of Geophysical Research: Atmospheres*, 110(D21), n/a-n/a, doi:10.1029/2005JD006111.
- Niu, G.-Y., Z.-L. Yang, R. E. Dickinson, L. E. Gulden, and H. Su (2007), Development of a simple groundwater model for use in climate models and evaluation with Gravity Recovery and Climate Experiment data, *Journal of Geophysical Research: Atmospheres*, 112(D7), n/a-n/a, doi:10.1029/2006JD007522.
- Oleson, K. W., et al. (2013), Technical Description of version 4.5 of the Community Land Model (CLM) *Rep. Ncar Technical Note NCAR/TN-503+STR*, National Center for Atmospheric Research, Boulder, CO.
- Pau, G. S. H., G. Bisht, and W. J. Riley (2014), A reduced-order modeling approach to represent subgrid-scale hydrological dynamics for land-surface simulations: application in a polygonal tundra landscape, *Geosci. Model Dev.*, 7(5), 2091-2105, doi:10.5194/gmd-7-2091-2014.
- Pau, G. S. H., C. Shen, W. J. Riley, and Y. Liu (2016), Accurate and efficient prediction of fine-resolution hydrologic and carbon dynamic simulations from coarse-resolution models, *Water Resources Research*, 52(2), 791-812, doi:10.1002/2015WR017782.
- Rahman, M., M. Sulis, and S. J. Kollet (2015), The subsurface-land surface-atmosphere connection under convective conditions, *Advances in Water Resources*, 83, 240-249, doi:10.1016/j.advwatres.2015.06.003.
- Rihani, J. F., F. K. Chow, and R. M. Maxwell (2015), Isolating effects of terrain and soil moisture heterogeneity on the atmospheric boundary layer: Idealized simulations to diagnose land-atmosphere feedbacks, *Journal of Advances in Modeling Earth Systems*, 7(2), 915-937, doi:10.1002/2014MS000371.
- Riley, W. J., and C. Shen (2014), Characterizing coarse-resolution watershed soil moisture heterogeneity using fine-scale simulations, *Hydrol. Earth Syst. Sci.*, 18(7), 2463-2483, doi:10.5194/hess-18-2463-2014.
- [Sakaguchi, K., and Zeng, X.: Effects of soil wetness, plant litter, and under-canopy atmospheric stability on ground evaporation in the Community Land Model \(CLM3.5\), \*Journal of Geophysical Research: Atmospheres\*, 114, n/a-n/a, 10.1029/2008JD010834, 2009.](#)
- Schaller, M. F., and Y. Fan (2009), River basins as groundwater exporters and importers: Implications for water cycle and climate modeling, *Journal of Geophysical Research: Atmospheres*, 114(D4), n/a-n/a, doi:10.1029/2008JD010636.
- Shen, C., J. Niu, and M. S. Phanikumar (2013), Evaluating controls on coupled hydrologic and vegetation dynamics in a humid continental climate watershed using a subsurface-land surface processes model, *Water Resources Research*, 49(5), 2552-2572, doi:10.1002/wrcr.20189.

Shen, C., W. J. Riley, K. M. Smithgall, J. M. Melack, and K. Fang (2016), The fan of influence of streams and channel feedbacks to simulated water and carbon fluxes, *Water Resources Research*, doi:10.1002/2015WR018086.

Shi, Y., K. J. Davis, C. J. Duffy, and X. Yu (2013), Development of a Coupled Land Surface Hydrologic Model and Evaluation at a Critical Zone Observatory, *Journal of Hydrometeorology*, 14(5), 1401-1420, doi:10.1175/JHM-D-12-0145.1.

[Shrestha, P., Sulis, M., Masbou, M., Kollet, S., and Simmer, C.: A Scale-Consistent Terrestrial Systems Modeling Platform Based on COSMO, CLM, and ParFlow, \*Monthly Weather Review\*, 142, 3466-3483, 10.1175/mwr-d-14-00029.1, 2014.](#)

[Sulis, M., Williams, J. L., Shrestha, P., Diederich, M., Simmer, C., Kollet, S. J., and Maxwell, R. M.: Coupling Groundwater, Vegetation, and Atmospheric Processes: A Comparison of Two Integrated Models, \*Journal of Hydrometeorology\*, 18, 1489-1511, 10.1175/jhm-d-16-0159.1, 2017.](#)

[Swenson, S. C., and Lawrence, D. M.: Assessing a dry surface layer-based soil resistance parameterization for the Community Land Model using GRACE and FLUXNET-MTE data, \*Journal of Geophysical Research: Atmospheres\*, 119, 10,299-210,312, 10.1002/2014JD022314, 2014.](#)

Tang, G., Yuan, F., Bisht, G., Hammond, G. E., Lichtner, P. C., Kumar, J., Mills, R. T., Xu, X., Andre, B., Hoffman, F. M., Painter, S. L., and Thornton, P. E.: Addressing numerical challenges in introducing a reactive transport code into a land surface model: a biogeochemical modeling proof-of-concept with CLM–PFLOTRAN 1.0, *Geosci. Model Dev.*, 9, 927-946, 10.5194/gmd-9-927-2016, 2016.

[Tang, J., and Riley, W. J. \(2013a\) Impacts of a new bare-soil evaporation formulation on site, regional, and global surface energy and water budgets in CLM4, \*Journal of Advances in Modeling Earth Systems\*, 5, 558-571, 10.1002/jame.20034, 2013a.](#)

[Tang, J. Y., and Riley, W. J. \(2013b\) A new top boundary condition for modeling surface diffusive exchange of a generic volatile tracer: theoretical analysis and application to soil evaporation, \*Hydrol. Earth Syst. Sci.\*, 17, 873-893, 10.5194/hess-17-873-2013, 2013b.](#)

Taylor, R. G., et al. (2013), Ground water and climate change, *Nature Clim. Change*, 3(4), 322-329.

Thorne, P. D., M. P. Bergeron, M. D. Williams, and V. L. Freedman (2006), Groundwater Data Package for Hanford Assessments *Rep. PNNL-14753*, Pacific Northwest National Laboratory, Richland, WA.

Tiffan, K. F., R. D. Garland, and D. W. Rondorf (2002), Quantifying flow-dependent changes in subyearling fall chinook salmon rearing habitat using two-dimensional spatially explicit modeling, *North American Journal of Fisheries Management*, 22(3), 713-726, doi:Doi 10.1577/1548-8675(2002)022<0713:Qfdcis>2.0.Co;2.

van Genuchten, M. T. (1980), A Closed-form Equation for Predicting the Hydraulic Conductivity of Unsaturated Soils1, *Soil Science Society of America Journal*, 44(5), 892-898, doi:10.2136/sssaj1980.03615995004400050002x.

Waichler, S. R., W. A. Perkins, and M. C. Richmond (2005), Hydrodynamic Simulation of the Columbia River, Hanford Reach, 1940-2004 *Rep. PNNL-15226*, Pacific Northwest National Laboratory, Richland, WA.

Williams, M. D., M. L. Rockhold, P. D. Thorne, and Y. Chen (2008), Three-Dimensional Groundwater Models of the 300 Area at the Hanford Site, Washington State *Rep. PNNL-17708*, Pacific Northwest National Laboratory, Richland, WA.

Wood, E. F., D. P. Lettenmaier, and V. G. Zartarian (1992), A land-surface hydrology parameterization with subgrid variability for general circulation models, *Journal of Geophysical Research: Atmospheres*, 97(D3), 2717-2728, doi:10.1029/91JD01786.

Xu, X., et al. (2016), A multi-scale comparison of modeled and observed seasonal methane emissions in northern wetlands, *Biogeosciences*, 13(17), 5043-5056, doi:10.5194/bg-13-5043-2016.

[Zachara, J. M., Chen, X., Murray, C., and Hammond, G. \(2016\). River stage influences on uranium transport in a hydrologically dynamic groundwater-surface water transition zone, \*Water Resources Research\*, 52, 1568-1590, 10.1002/2015WR018009, 2016.](#)

[Zeng, X., Zhao, M., and Dickinson, R. E. \(1998\), Intercomparison of bulk aerodynamic algorithms for the computation of sea surface fluxes using TOGA COARE and TAO data, \*Journal of Climate\*, 11, 2628-2644, 1998.](#)

[Zeng, X., Dickinson, R. E., Barlage, M., Dai, Y., Wang, G., and Oleson, K. \(2005\), Treatment of undercanopy turbulence in land models, \*Journal of Climate\*, 18, 5086-5094, 10.1175/JCLI3595.1.](#)

[Zeng, X., and Wang, A. \(2007\), Consistent Parameterization of Roughness Length and Displacement Height for Sparse and Dense Canopies in Land Models, \*Journal of Hydrometeorology\*, 8, 730-737, 10.1175/jhm607.1.](#)

[Zeng, X., and Decker, M. \(2009\), Improving the Numerical Solution of Soil Moisture-Based Richards Equation for Land Models with a Deep or Shallow Water Table, \*Journal of Hydrometeorology\*, 10, 308-319, 10.1175/2008JHM1011.1.](#)

Zhang, B., J. L. Tang, C. Gao, and H. Zepp (2011), Subsurface lateral flow from hillslope and its contribution to nitrate loading in streams through an agricultural catchment during subtropical rainstorm events, *Hydrol. Earth Syst. Sci.*, 15(10), 3153-3170, doi:10.5194/hess-15-3153-2011.

Zhou, T., B. Nijssen, H. L. Gao, and D. P. Lettenmaier (2016), The Contribution of Reservoirs to Global Land Surface Water Storage Variations, *Journal of Hydrometeorology*, 17(1), 309-325, doi:10.1175/jhm-d-15-0002.1.

## Tables and Figures

Table 1. Summary of numerical experiments

<b>Experiments</b>	<b><a href="#">Model</a></b>	<b>Horizontal Resolution</b>	<b>Lateral flow</b>	<b>River Stage (m)</b>
<a href="#">PFCLM<sub>v2m</sub>S<sub>v2m</sub></a>	<a href="#">CP v1.0</a>	2m	No	Observed
<a href="#">PFCLM<sub>2m</sub>S<sub>2m</sub></a>	<a href="#">CP v1.0</a>	2m	Yes	Observed
<a href="#">PFCLM<sub>10m</sub>S<sub>10m</sub></a>	<a href="#">CP v1.0</a>	10m	Yes	Observed
<a href="#">PFCLM<sub>20m</sub>S<sub>20m</sub></a>	<a href="#">CP v1.0</a>	20m	Yes	Observed
<a href="#">PFCLM<sub>E2m</sub>S<sub>E2m</sub></a>	<a href="#">CP v1.0</a>	2m	Yes	Observed +5
<a href="#">PFCLM<sub>E10m</sub>S<sub>E10m</sub></a>	<a href="#">CP v1.0</a>	10m	Yes	Observed +5
<a href="#">PFCLM<sub>E20m</sub>S<sub>E20m</sub></a>	<a href="#">CP v1.0</a>	20m	Yes	Observed +5
<a href="#">CLM<sub>2m</sub></a>	<a href="#">CLM4.5</a>	<a href="#">2m</a>	<a href="#">No</a>	<a href="#">Not applicable</a>

Table 2. Hydrogeological material properties of Hanford and Ringold materials.

Material	Porosity	Permeability (m <sup>2</sup> )	Van Genuchten/Burdine Parameters		
			Res. Sat.	m	alpha
<b>Hanford</b>	0.20	$7.387 \times 10^{-9}$	0.16	0.34	$7.27 \times 10^{-4}$
<b>Ringold</b>	0.40	$1.055 \times 10^{-12}$	0.13	0.75	$1.43 \times 10^{-4}$

Table 3. The comparison between simulated and observed water table levels

Well number	<u>PFCLM<sub>2m</sub>S<sub>2m</sub></u>		<u>PFCLM<sub>10m</sub>S<sub>10m</sub></u>		<u>PFCLM<sub>20m</sub>S<sub>20m</sub></u>	
	RMSE (m)	N-S	RMSE (m)	N-S	RMSE (m)	N-S
<b>399-3-29</b>	0.022	0.999	0.022	0.999	0.021	0.999
<b>399-3-34</b>	0.011	1.000	0.011	1.000	0.006	1.000
<b>399-2-01</b>	0.039	0.997	0.038	0.997	0.029	0.998
<b>399-1-60</b>	0.016	1.000	0.016	0.999	0.013	1.000
<b>399-2-33</b>	0.028	0.998	0.028	0.998	0.022	0.999
<b>399-1-21A</b>	0.023	0.999	0.023	0.999	0.020	0.999
<b>399-2-03</b>	0.037	0.997	0.037	0.997	0.029	0.998
<b>399-2-02</b>	0.045	0.995	0.045	0.995	0.042	0.996
<b>mean</b>	0.028	0.998	0.028	0.998	0.023	0.999

Table 4. The relative error in surface energy fluxes simulated by [PFCLM<sub>v2m-Sv2m</sub>](#) and [PFCLM<sub>10m-S10m</sub>](#) benchmarked against [PFCLM<sub>2m-S2m</sub>](#) and by [PFCLM<sub>E10m-SE10m</sub>](#) and [PFCLM<sub>E20m-SE20m</sub>](#) benchmarked against [PFCLM<sub>E2m-SE2m</sub>](#)

<b>Simulation</b>	<b>Latent heat flux (%)</b>	<b>Sensible heat flux (%)</b>
<a href="#">PFCLM<sub>v2m-Sv2m</sub></a>	5.67	1.63
<a href="#">PFCLM<sub>10m-S10m</sub></a>	1.35	0.78
<a href="#">PFCLM<sub>20m-S20m</sub></a>	2.41	1.42
<a href="#">PFCLM<sub>E10m-SE10m</sub></a>	33.19	13.71
<a href="#">PFCLM<sub>E20m-SE20m</sub></a>	33.84	14.18

Table 5. The relative error in total water mass and tracer amount in the subsurface simulated by [in PFCLM<sub>40m-S10m</sub>](#) and [PFCLM<sub>20m-S20m</sub>](#) benchmarked against [PFCLM<sub>2m-S2m</sub>](#) and by [PFCLM<sub>E40m-SE10m</sub>](#) and [PFCLM<sub>E20m-SE20m</sub>](#) benchmarked against [PFCLM<sub>E2m-SE2m</sub>](#)

<b>Simulation</b>	Total water mass (%)	Total tracer (%)
<a href="#">PFCLM<sub>40m-S10m</sub></a>	0.03	5.44
<a href="#">PFCLM<sub>20m-S20m</sub></a>	0.04	10.40
<a href="#">PFCLM<sub>E40m-SE10m</sub></a>	9.87	22.00
<a href="#">PFCLM<sub>E20m-SE20m</sub></a>	9.85	22.00

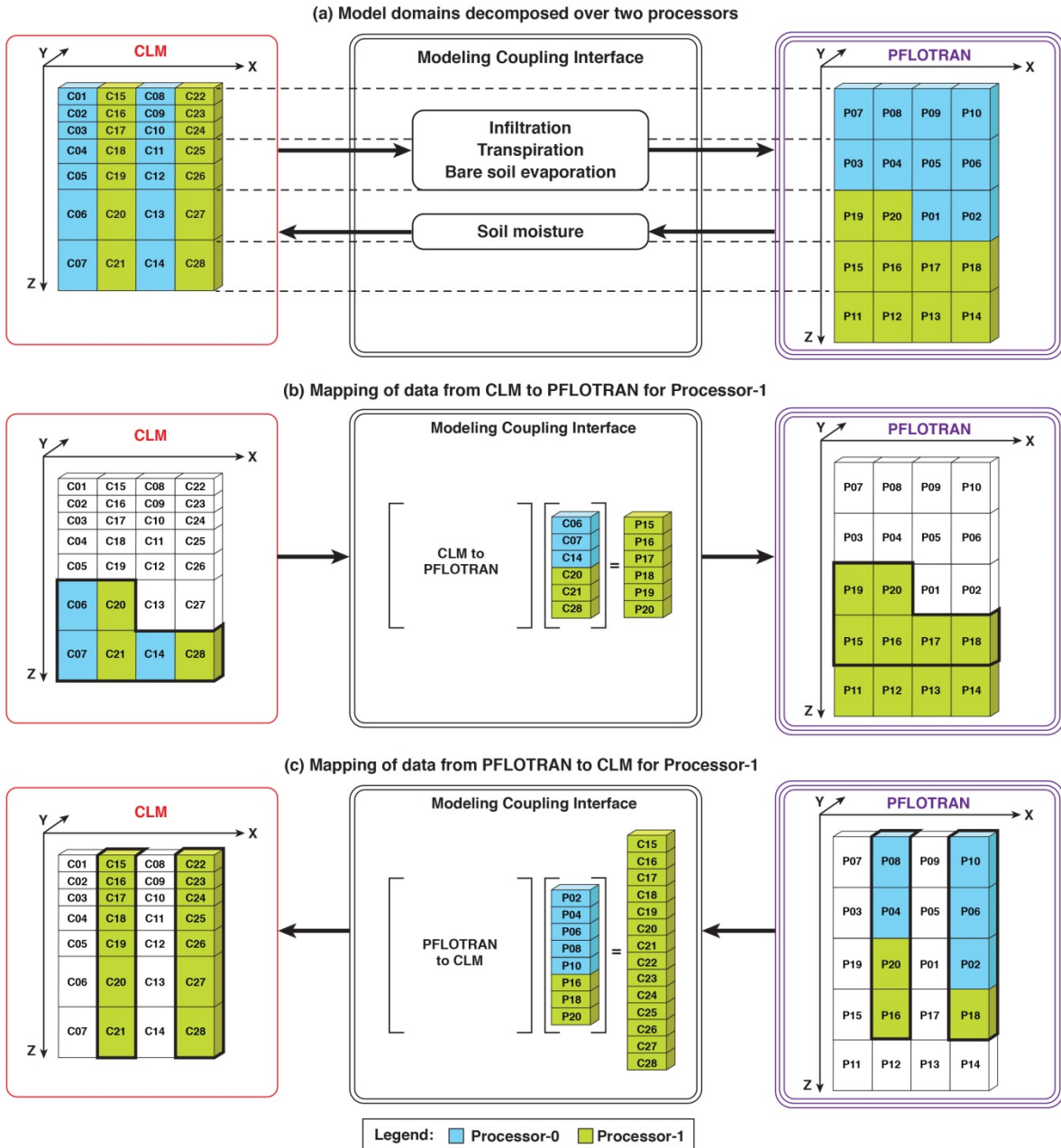


Figure 1. Schematic representations of the model coupling interface of CP v1.0. (a) Domain decomposition of a hypothetical CLM and PFLOTRAN domain comprising of 4x1x7 and 4x1x5 grids in x, y, and z directions across two processors as shown in blue and green. (b) Mapping of water fluxes from CLM onto PFLOTRAN domain via a local sparse matrix vector product for grids on processor 1. (c) Mapping of updated soil moisture from PFLOTRAN onto CLM domain via a local sparse matrix vector product for grids on processor 1.

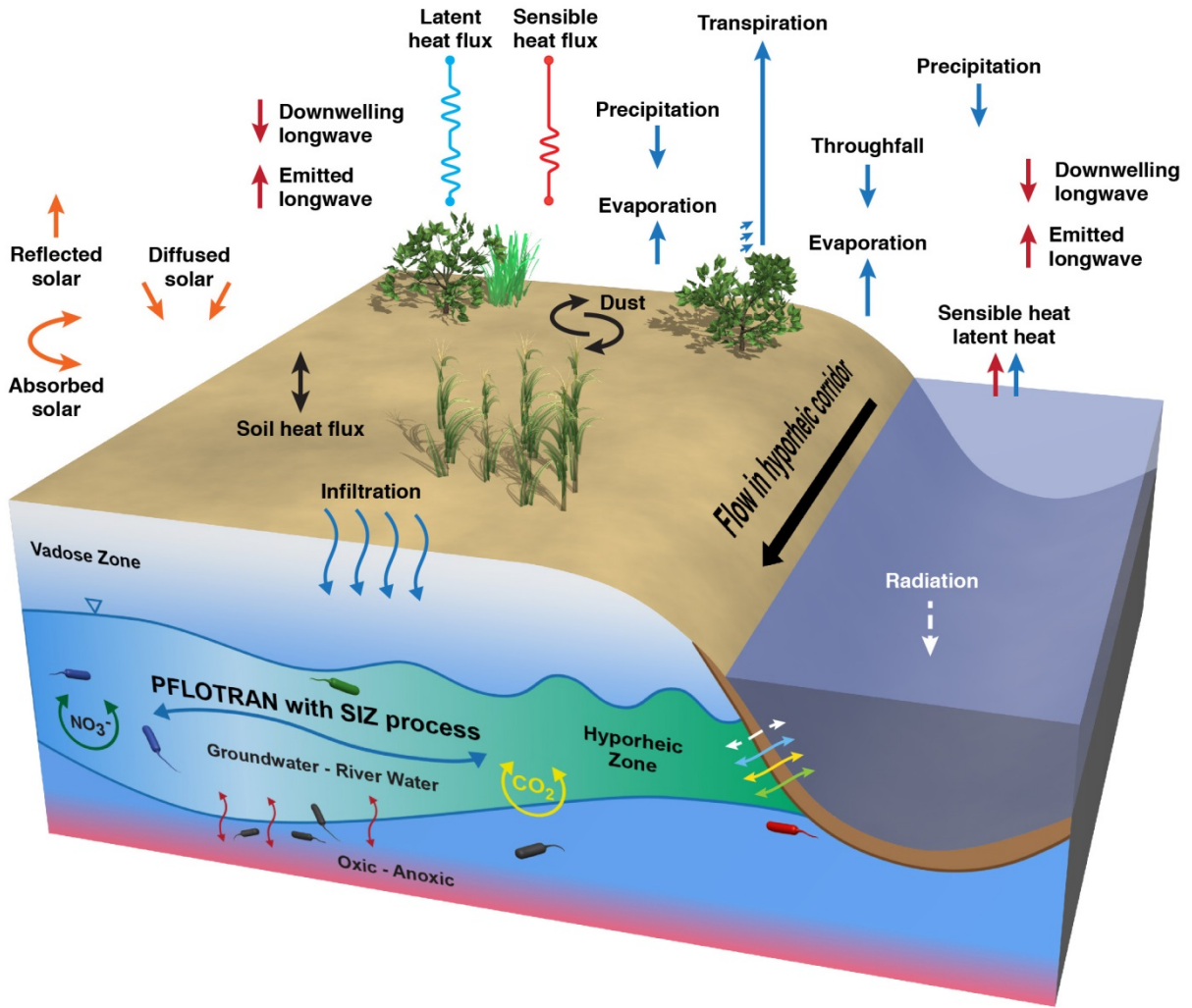


Figure 2. Schematic representation of hydrologic processes simulated in CP v1.0

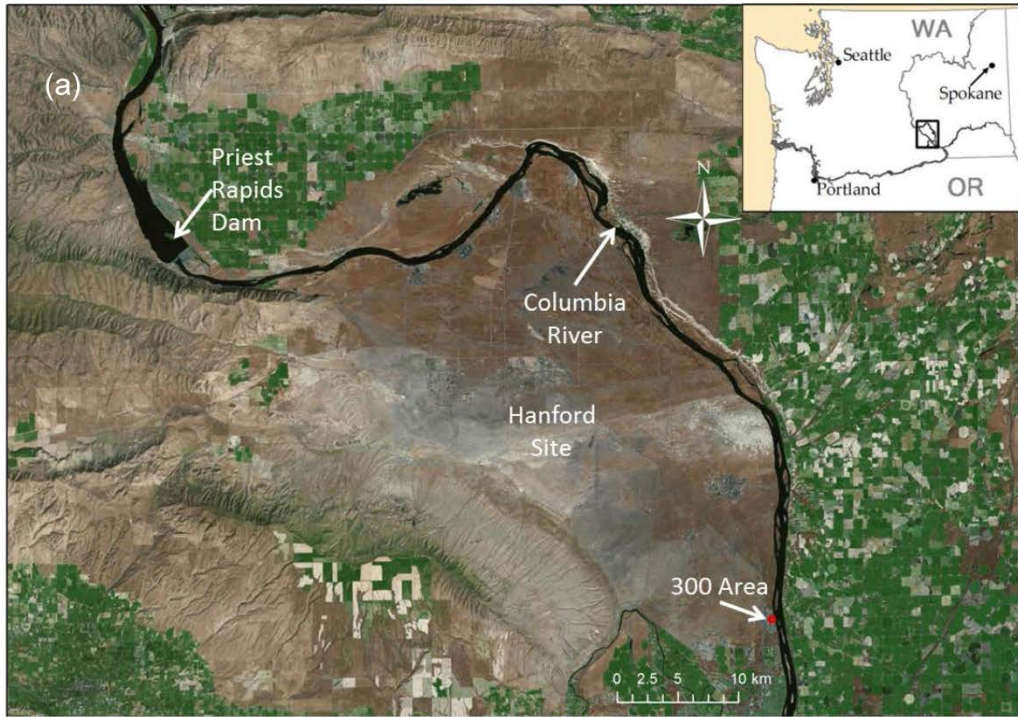


Figure 23. (Top) The Hanford Reach of the Columbia River and the Hanford Site location in south-central Washington State, USA; (Bottom) the 400 m x 400 m modeling domain located in the Hanford 300 Area.

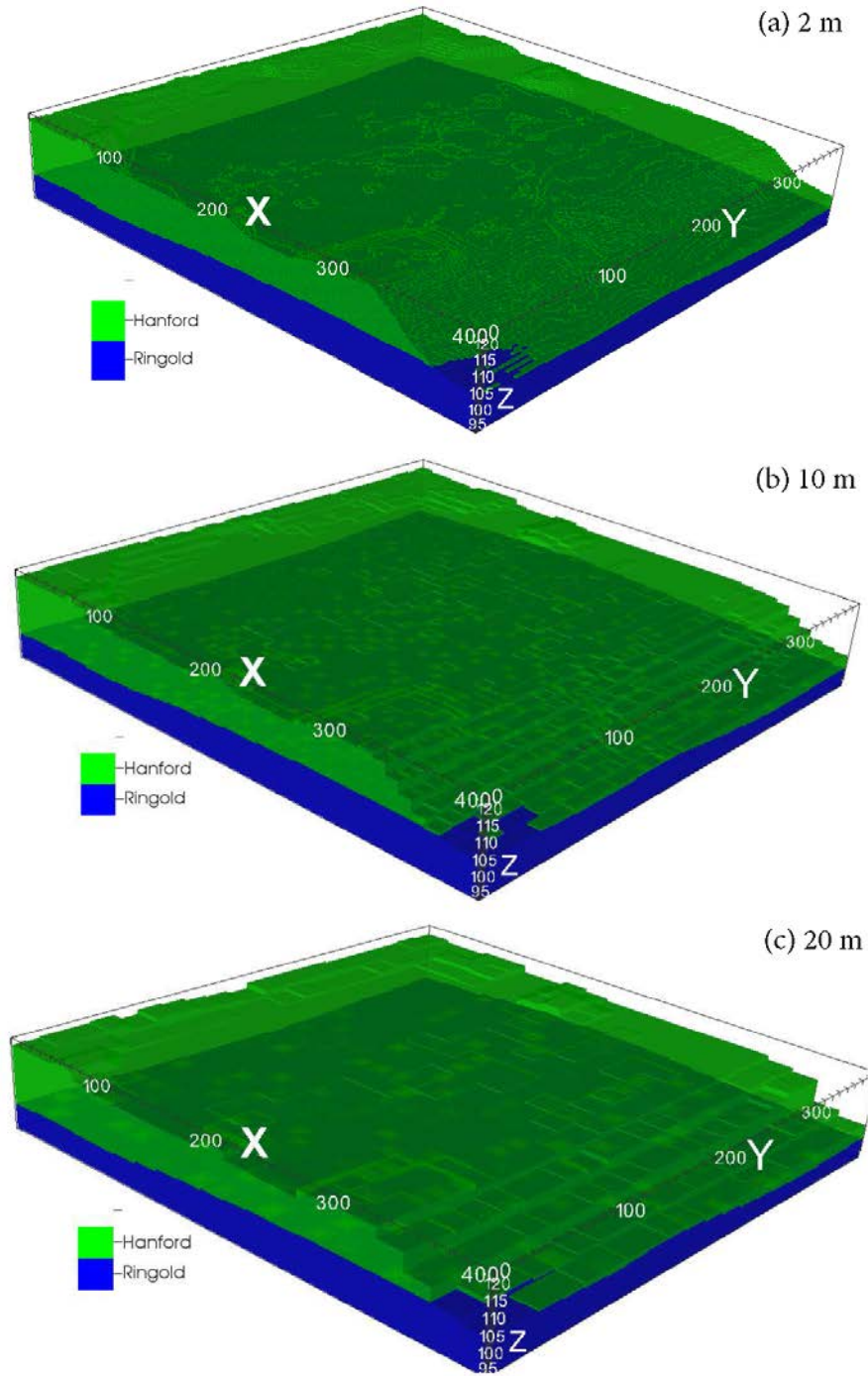


Figure 34. PFLOTRAN meshes and associated material IDs at (a) 2-m; (b) 10-m; and (c) 20-m resolutions

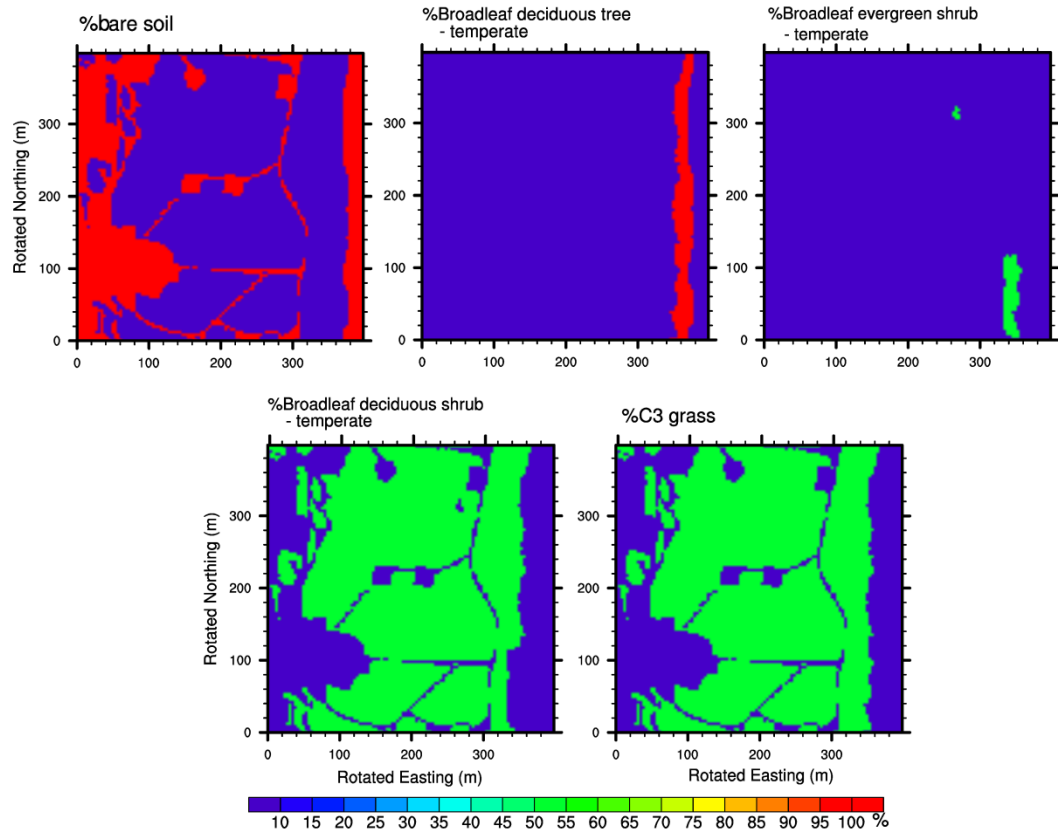


Figure 45. Plant function types at 2-m resolution as inputs for CLM4.5

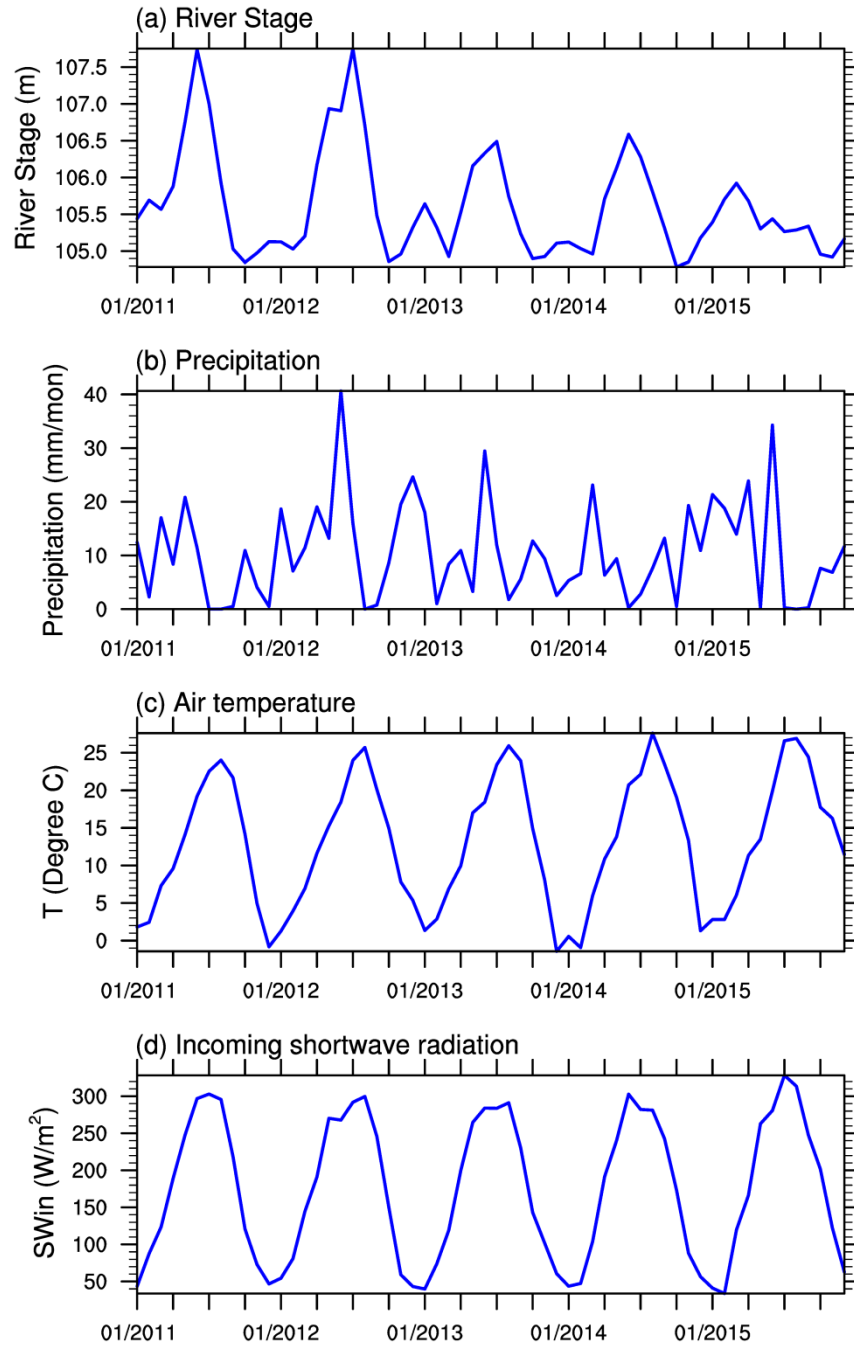
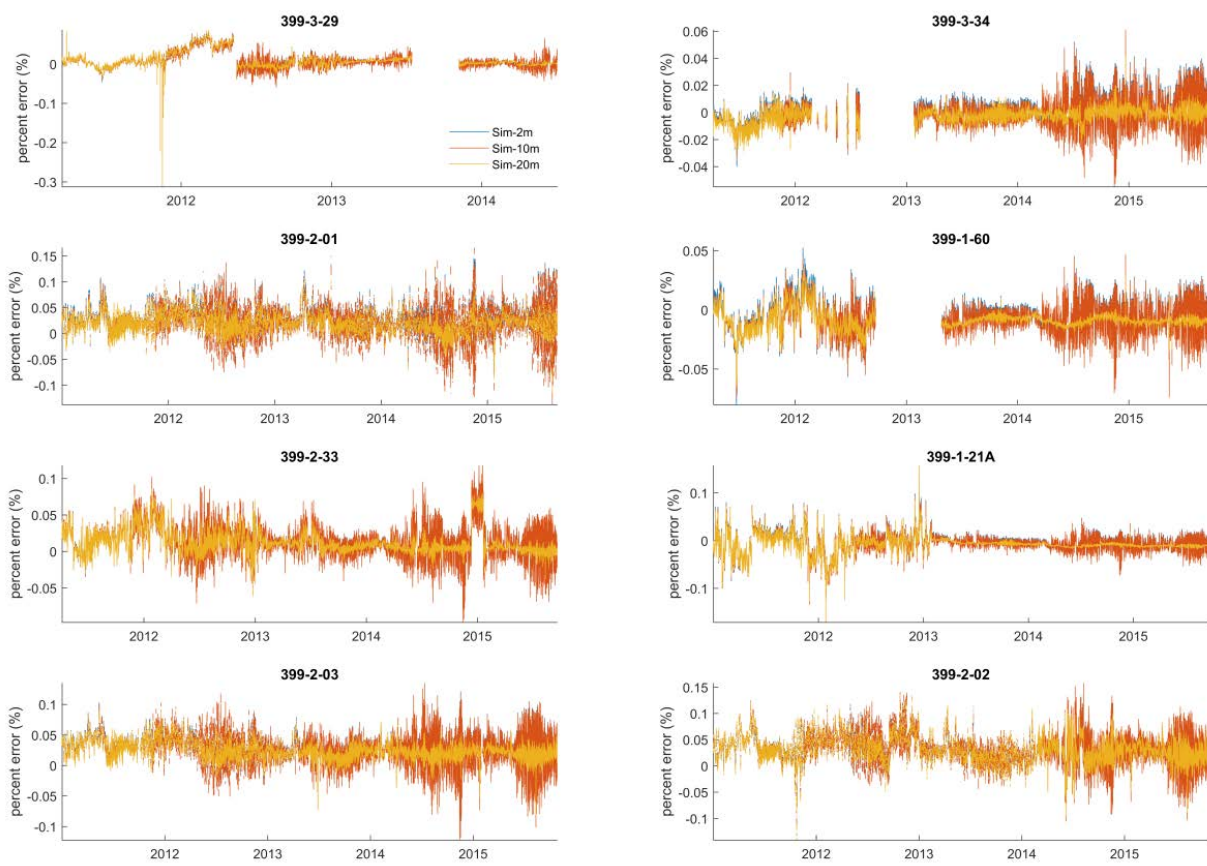


Figure 56. Hydro-meteorological drivers in the study period: (a) monthly mean river Stage; (b) monthly total precipitation; (c) monthly mean surface air temperature; (d) and monthly mean incoming shortwave radiation.



[Figure 7. Deviation \(in percentages\) of simulated water table levels from observations at selected wells shown in Figure 3b.](#)

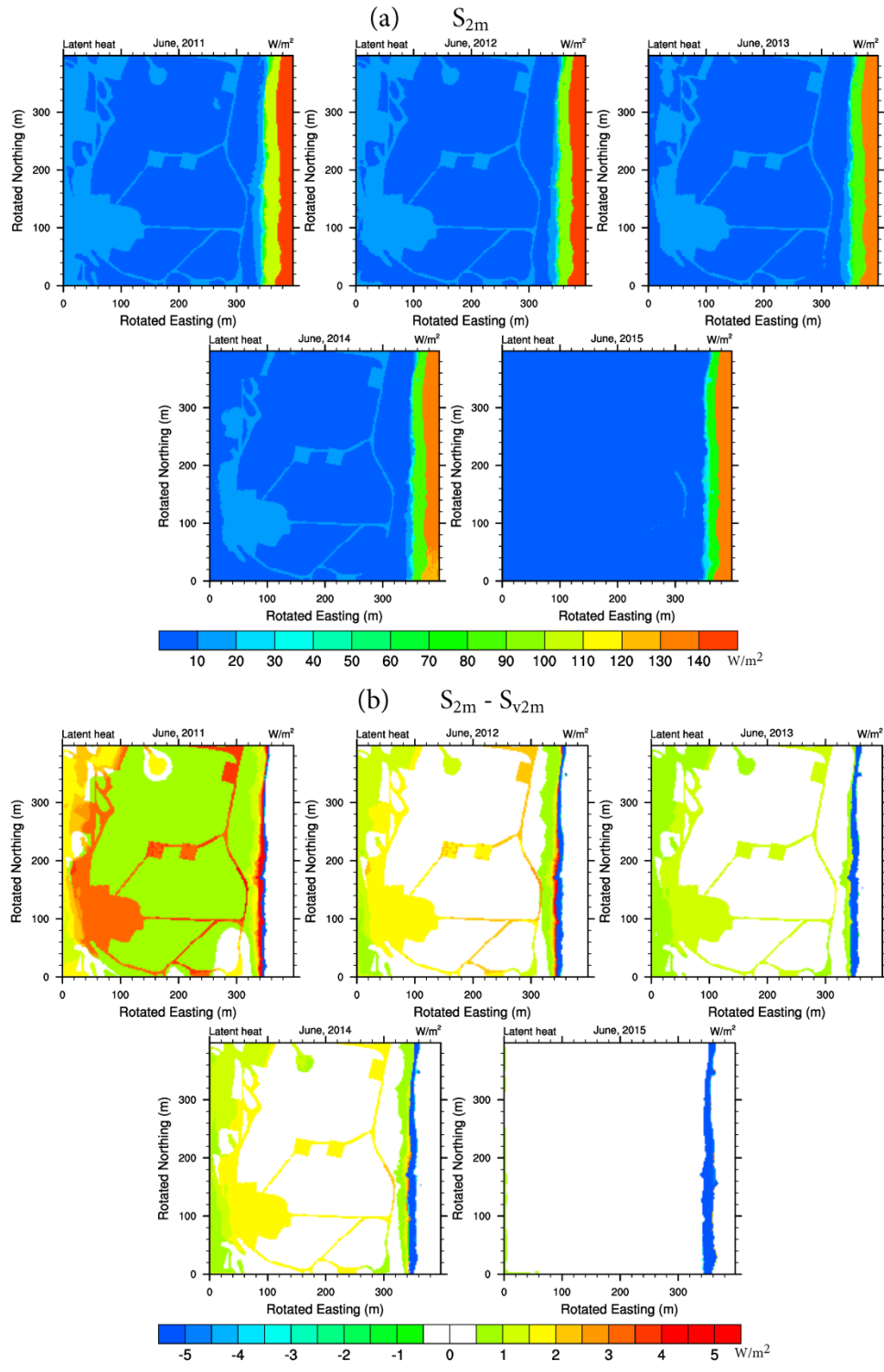


Figure 78. (a) Simulated latent heat fluxes in June from the 3-D simulation ( $PFCLM2mS_{2m}$ ); and (b) the difference between the 3-D and vertical only simulations (i.e.,  $PFCLM2mS_{2m} - PFCLMv2mS_{v2m}$ ).

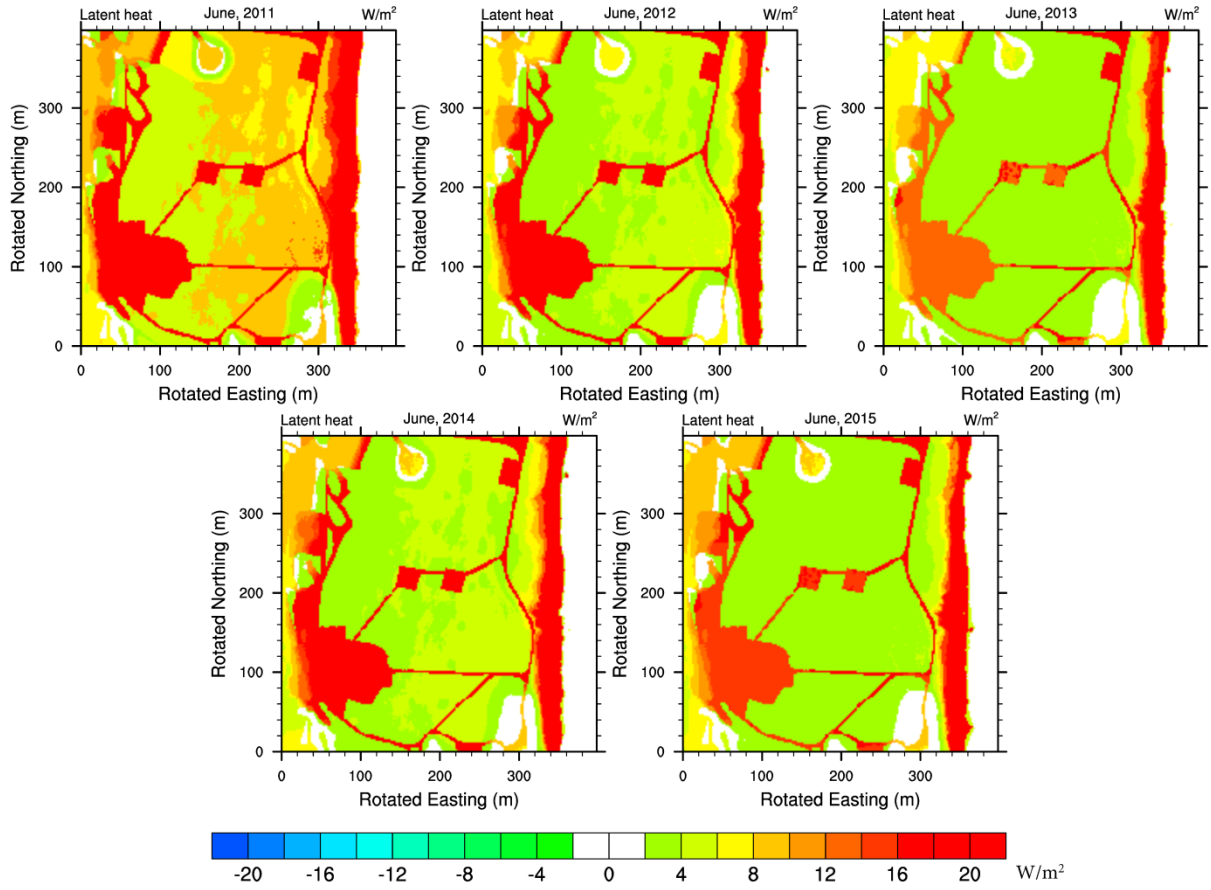


Figure 89. Difference between simulated latent heat fluxes in June from PFCLM<sub>E2m</sub> between by S<sub>E2m</sub> and S<sub>2m</sub> in June.

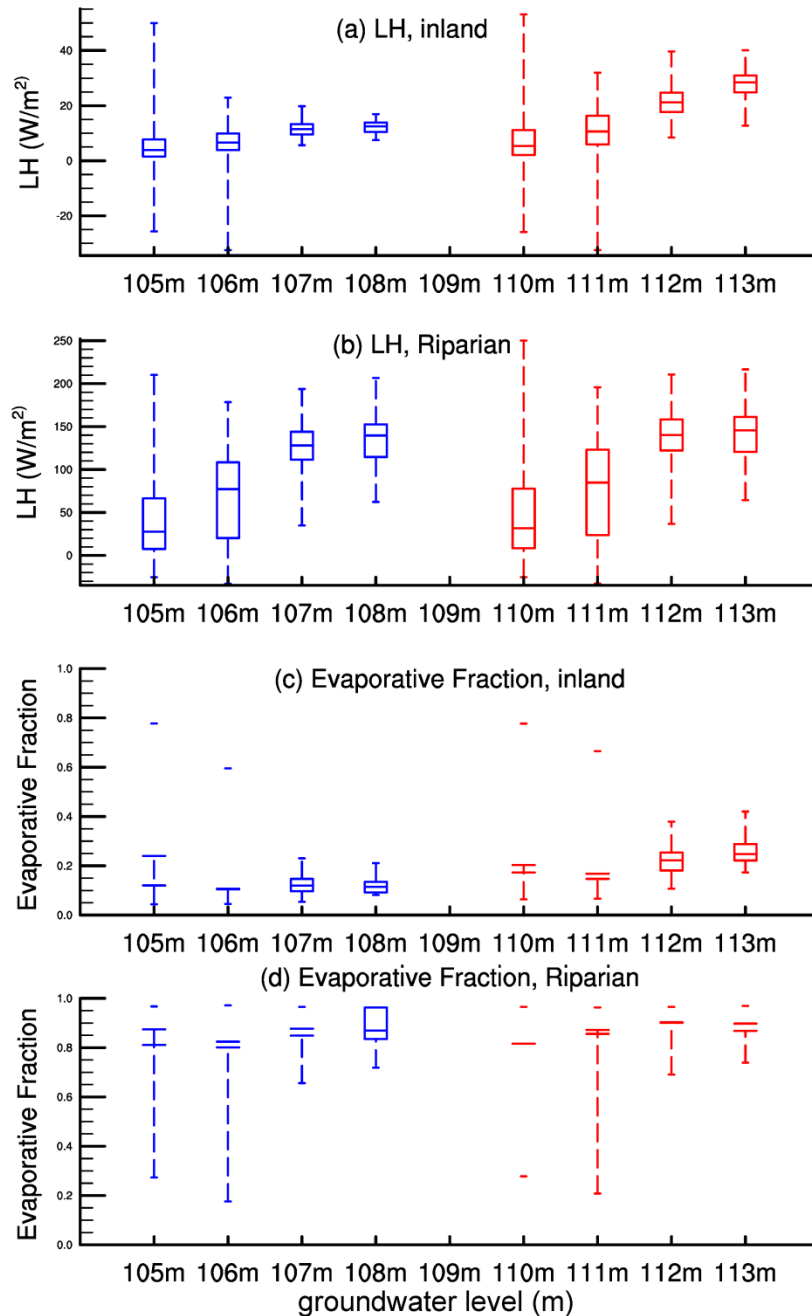


Figure 910. Boxplots of (a) land heat fluxes over the inland domain; (b) and latent heat fluxes in the riparian zone; (c) Bowen ratios/evaporative fractions over the inland domain; (d) Bowen ratios/evaporative fractions in the riparian zone in relation to groundwater table levels in the warm month (April to September) in the five-year period. The red boxes and whiskers represent summary statistics from PFCLM<sub>E2m</sub>S<sub>E2m</sub>, and red ones indicate those from PFCLM<sub>E2m</sub>S<sub>E2m</sub>. The bottom and top of each box are the 25<sup>th</sup> and 75<sup>th</sup> percentile, the band inside the box is median, and the ends of the whiskers are maximum and minimum values, respectively.

### Transect, y=200m

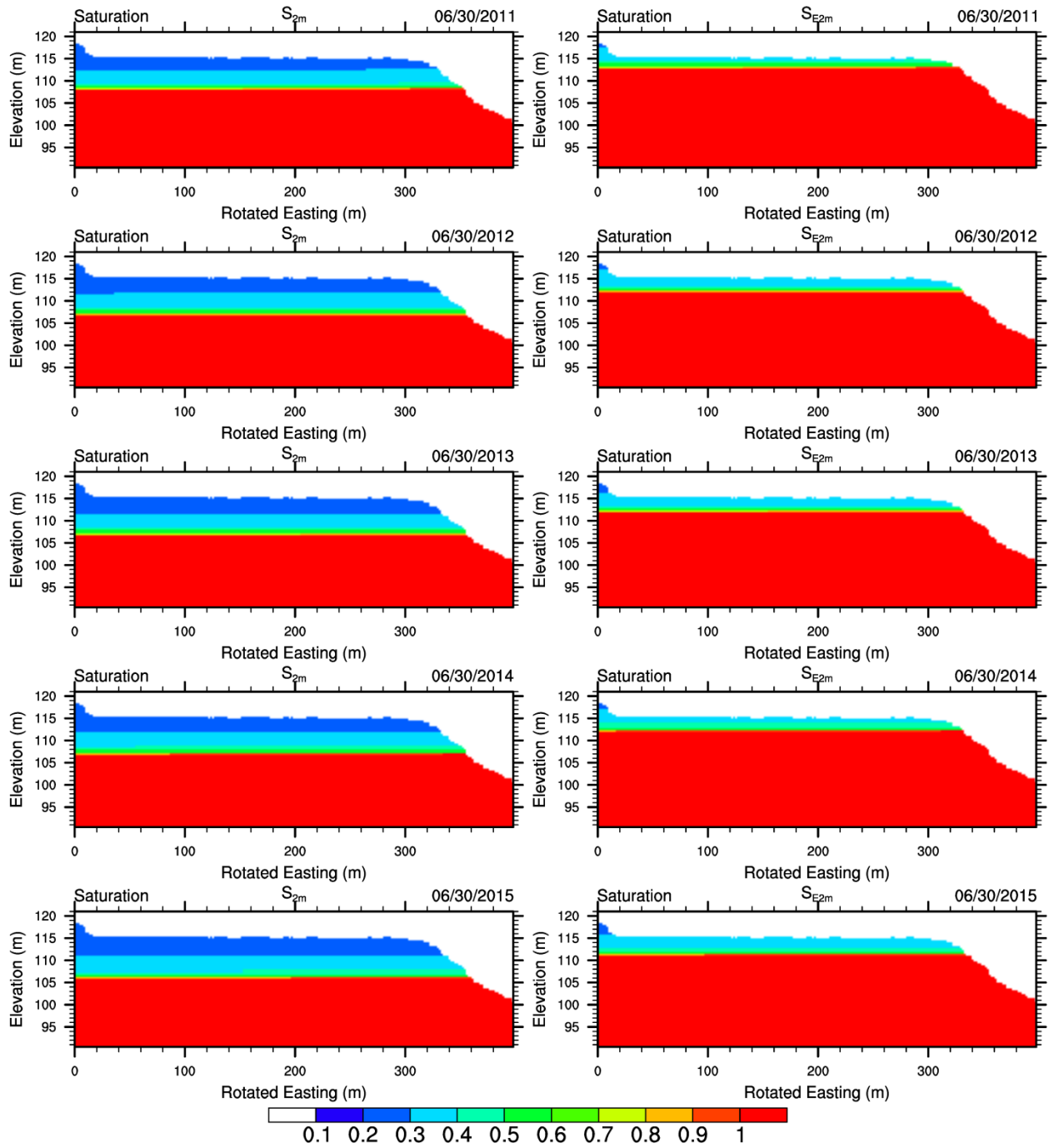


Figure 4011. Liquid saturation levels (unitless) across a transect perpendicular to the river ( $y=200m$ ) on 30 June of each year in the study period from (a)  $PFCLM_{S_{2m}}$  and (b)  $PFCLM_{E_{2m}}$

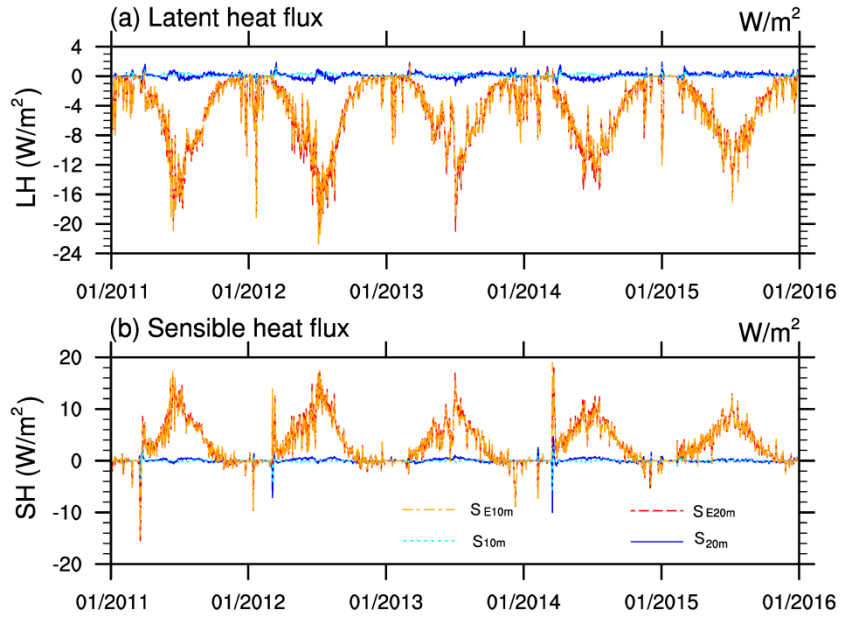


Figure 4412. Deviations of simulated domain-average latent heat and sensible heat fluxes from those simulated by  $PFCLM_{E2m-S2m}$  (for  $PFCLM_{E10m-S10m}$  and  $PFCLM_{E20m-S20m}$ ), and by  $PFCLM_{E2m-SE2m}$  (for  $PFCLM_{E10m-SE10m}$  and  $PFCLM_{E20m-SE20m}$ ).

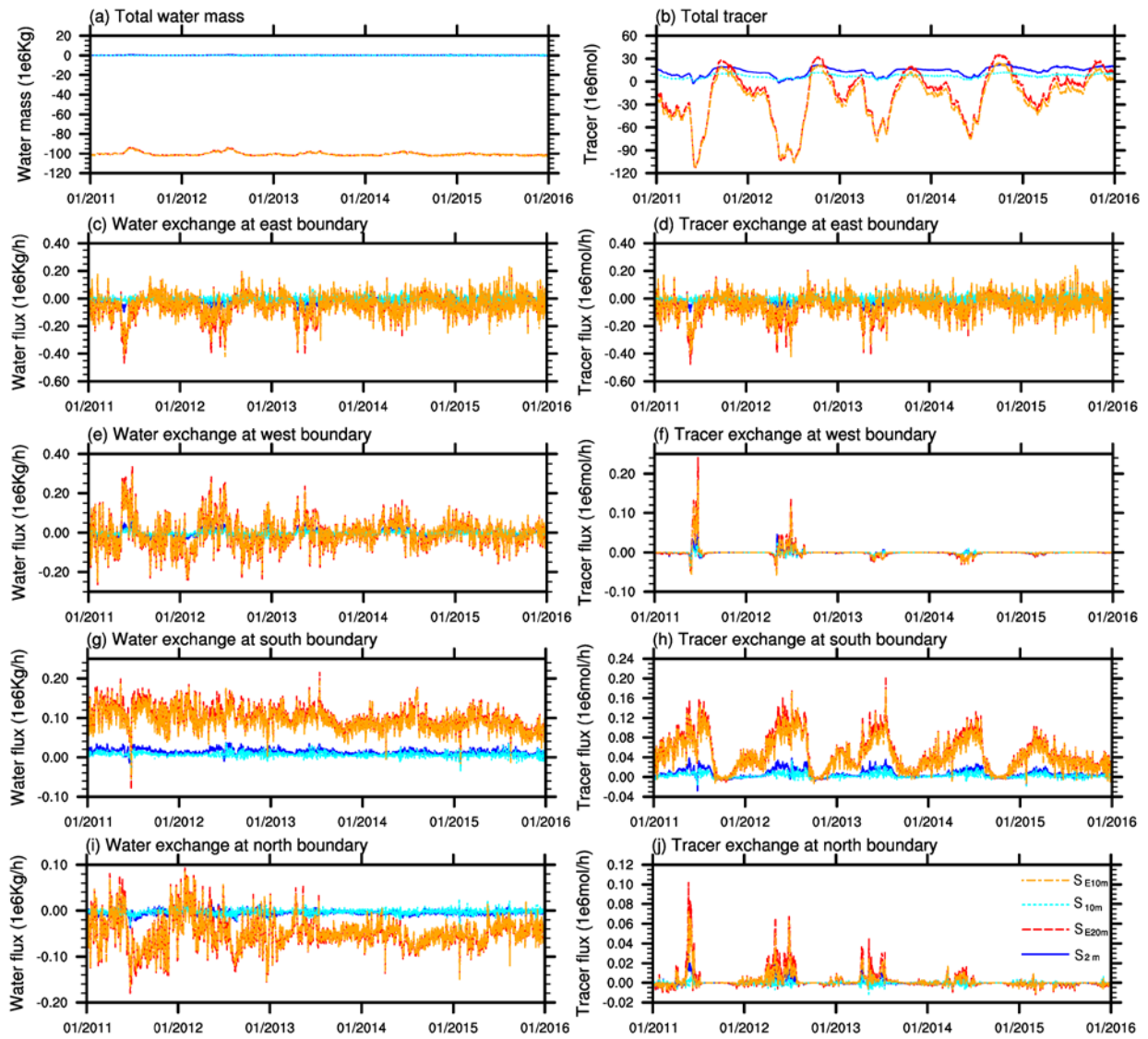


Figure 4213. Deviations of total water mass, tracer, and exchange rates of water and tracer at four boundaries from those simulated by  $PFCLM_{2m}-S_{2m}$  (for  $PFCLM_{10m}-S_{10m}$  and  $PFCLM_{20m}-S_{20m}$ ), and by  $PFCLM_{E2m}-S_{E2m}$  (for  $PFCLM_{E10m}-S_{E10m}$  and  $PFCLM_{E20m}-S_{E20m}$ ).